NUMERICAL AND EXPERIMENTAL ANALYSIS OF DISSIPATIVE SILENCER COUPLED WITH QUARTER WAVE TUBE

A THESIS SUBMITTED TO
THE GRADUATE SCHOOL OF NATURAL AND APPLIED SCIENCES
OF
MIDDLE EAST TECHNICAL UNIVERSITY

BY

AYŞE DİNÇER

IN PARTIAL FULLFILLMENT OF THE REQUIREMENTS
FOR
THE DEGREE OF MASTER OF SCIENCE
IN
MECHANICAL ENGINEERING

JANUARY 2013

Approval of the thesis:

NUMERICAL AND EXPERIMENTAL ANALYSIS OF DISSIPATIVE SILENCER COUPLED WITH QUARTER WAVE TUBE

submitted by **AYŞE DİNÇER** in partial fulfillment of the requirements for the degree of **Master of Science in Mechanical Engineering Department, Middle East Technical University** by,

Prof. Dr. Canan ÖZGEN
Dean, Graduate School of **Natural and Applied Sciences** _____

Prof. Dr. Süha ORAL
Head of Department, **Mechanical Engineering** _____

Prof. Dr. Mehmet ÇALIŞKAN
Supervisor, **Mechanical Engineering Dept., METU** _____

Examining Committee Members:

Prof. Dr. M. Haluk AKSEL
Mechanical Engineering Dept., METU _____

Prof. Dr. Mehmet ÇALIŞKAN
Mechanical Engineering Dept., METU _____

Prof. Dr. Yusuf ÖZYÖRÜK
Aerospace Engineering Dept., METU _____

Asst. Prof. M. Metin YAVUZ
Mechanical Engineering Dept., METU _____

Uğur ETİZ, M.Sc.
REHİS, ASELSAN _____

Date: **25.01.2013**

I hereby declare that all information in this document has been obtained and presented in accordance with academic rules and ethical conduct. I also declare that, as required by these rules and conduct, I have fully cited and referenced all material and results that are not original to this work.

Name, Last name : Ayşe DİNÇER

Signature :

ABSTRACT

NUMERICAL AND EXPERIMENTAL ANALYSIS OF DISSIPATIVE SILENCER COUPLED WITH QUARTER WAVE TUBE

DİNÇER, Ayşe
M. Sc., Department of Mechanical Engineering
Supervisor: Prof. Dr. Mehmet ÇALIŞKAN

January 2013, 56 pages

The study deals with investigation of acoustical characteristics of a hybrid silencer made up of a dissipative silencer and a quarter wave tube resonator. The theoretical and experimental analyses are performed to define acoustic characteristics of a simple expansion chamber and reactive perforated silencer, while the numerical and experimental solutions are presented for dissipative perforated silencer. Furthermore, the experiments and numerical solutions are extended to the hybrid silencer to find the effect of quarter wave tube resonator on the silencer performance. The experimental results of dissipative silencer are verified with theoretical solutions. The empirical expressions for acoustic impedance of perforation and filling material are presented in this study for use in a three-dimensional boundary element method (BEM). Besides, an experimental setup is also established to find the characteristic impedance and wavenumber of absorbing material to import BEM solution when the empirical expression cannot be used. The results found with BEM are compared by analytical and experimental results favorably.

Keywords: Dissipative silencer, quarter wave tube, transmission loss, Boundary Element Method

ÖZ

ÇEYREK DALGA TÜPÜ İLE BİRLEŞTİRİLMİŞ DAĞITICI SUSUTURUCUNUN SAYISAL VE DENEYSEL ANALİZİ

DİNÇER, Ayşe
Yüksek Lisans, Makina Mühendisliği Bölümü
Tez Yöneticisi: Prof. Dr. Mehmet ÇALIŞKAN

Ocak 2013, 56 Sayfa

Bu çalışma; dağıtıcı susturucu ve çeyrek dalga tüp rezonatörden oluşan melez bir susturucunun akustik karakteristiğinin incelenmesi ile ilgilidir. Basit genleşme haznesi ve reaktif delikli susturucunun akustik karakteristiği teorik ve deneysel yöntemlerle tanımlanırken, dağıtıcı delikli susturucunun kararketristiği sayısal ve deneysel çözümlerle ortaya konmaktadır. Ayrıca deneyler ve analitik çalışmalar çeyrek dalga tübünün susturucu performansına etkisini göstermek amacıyla melez susturucu için de genişletilmiştir. Dağıtıcı susturucunun deneysel sonuçları analitik çözümlerle doğrulanmıştır. Dolgu malzemesinin ve delikli yüzeyin akustik impedansının ampirik ifadeleri, üç boyutlu sınır eleman yönteminde kullanılmak üzere bu çalışmada sunulmaktadır. Ayrıca, ampirik ifadelerin kullanılamaması durumunda üç boyutlu sınır eleman yönteminde kullanılmak üzere dolgu malzemesinin karakteristik impedansı ve dalga boyunu bulmak amacıyla bir deney düzeneği daha kurulmuştur. Sınır eleman yönteminin sonuçları analitik ve deneysel sonuçlarla uygun bir şekilde karşılaştırılmıştır.

Anahtar Kelimeler: Dağıtıcı susturucu, çeyrek dalga tübü, iletim kaybı, Sınır Eleman Yöntemi

To My Husband
And
Our Beloved Families

ACKNOWLEDGEMENTS

I would like to express my gratitude to my supervisor Prof. Dr. Mehmet ÇALIŞKAN for his guidance, advice, criticism, encouragement and insight throughout the completion of the thesis.

I am indebted to all of my friends and colleagues, especially Fatih Dere, Uğur Etiz, Mustafa Berispek and Selçuk Öksüz, for their support and encouragements. I am also grateful to ASELSAN Inc. and AKA Kalıp for the facilities that made my work easier.

Finally, I am grateful to my husband, Onur Dinçer, and our families for their continuous support and encouragements.

TABLE OF CONTENTS

ABSTRACT ..... **v**
ÖZ ..... **vi**
ACKNOWLEDGEMENTS ..... **viii**
TABLE OF CONTENTS ..... **ix**
LIST OF FIGURES ..... **x**
LIST OF TABLES ..... **xii**
LIST OF ABBREVIATIONS ..... **xiii**
NOMENCLATURE ..... **xiv**
CHAPTERS **1**
1. INTRODUCTION **1**
1.1 Background 1
1.2 Thesis Organization 2
2. LITERATURE SURVEY **3**
2.1 Analytical Methods 3
2.2 Numerical Methods 4
2.3 Experimental Methods 5
3. THEORETICAL MODELS **7**
3.1 Acoustic Performance of Silencer 7
3.2 Acoustical Properties of Absorbing Material 12
3.2.1 Physical Properties of Absorbing Material 12
3.2.2 Acoustical Characterization of Absorbing Material 13
3.3 Acoustic Impedance of the Perforation 13
3.3.1 Acoustic Impedance of Air-Air Interaction 15
3.3.2 Acoustic Impedance of Air-Fibrous Interaction 15
3.4 Acoustic Performance of Quarter Wave Tube [26] 15
4. NUMERICAL MODELING **19**
4.1 Acoustic Properties of Perforation in VNoise 19
4.2 Acoustical Properties of Absorbing Material in VNoise 20
4.3 Evaluation of Transmission Loss and Insertion Loss in VNoise 20
4.4 Steps of the Numerical Solution of the Study 22
4.5 Properties of Numerical Model 23
5. TRANSMISSION LOSS MEASUREMENT **25**
5.1 Transmission Loss Measurement with Two Load Method [28] 25
5.2 Characteristic Impedance and Wavenumber Measurement with Two Load Method 28
5.3 Experimental Test Setup 29
5.3.1 Test Setup Specifications [30] 31
5.3.2 Calibration of the Microphones 33
5.4 Transmission Loss Measurements 34
5.4.1 Simple Expansion Chamber 34
5.4.2 Reactive Perforated Silencer 38
5.4.3 Dissipative Perforated Silencer 44
5.4.4 Hybrid Silencer 46
6. CONCLUSION **53**
6.1 Future Work 54
REFERENCES **55**

LIST OF FIGURES

FIGURES

Figure 1-1: Forced air cooling schemes for military electronics....1
Figure 2-1: The schematic view of a) expansion chamber (cavity) b) equivalent circuit of a cavity element. [3] 3
Figure 2-2: Test setup for Two Source Method [16] 6
Figure 2-3: Test setup for Two Load Method [16] 6
Figure 3-1: The schematic of a perforated dissipative single-pass straight silencer. 7
Figure 3-2: The mode shapes and zeros of derivatives of the Bessel Function [18] 8
Figure 3-3: Wave propagation through a perforated plate in a duct. [24] 13
Figure 3-4: The schematic view of QWT resonator 15
Figure 4-1: Transmission loss of a muffler with porosity 0.098, hole diameter 0.003175 and number holes 276 [24] 20
Figure 4-2: Schematic representation of a generic duct or muffler 21
Figure 4-3: Transmission loss of a simple expansion chamber with three different discretized models (6, 8 and 10 points per wave) 23
Figure 5-1: Transfer matrix between incident and reflecting waves 25
Figure 5-2: Schematic view of measurement setup of two load method 26
Figure 5-3: Schematic view of test setup with filling material test specimen 28
Figure 5-4: Schematic view of experimental test setup 30
Figure 5-5: The experimental test setup of the study. 31
Figure 5-6: Two examples of typical microphone mounting 32
Figure 5-7: Configuration for calibration of the microphones 33
Figure 5-8: The schematic view of simple expansion chamber 35
Figure 5-9: Magnitude of the calibration factor between microphones 35
Figure 5-10: Phase of the calibration factor between microphones 36
Figure 5-11: Test setup of the expansion chamber 36
Figure 5-12: BEM model of the simple expansion chamber 37
Figure 5-13: Transmission Loss of simple expansion chamber 37
Figure 5-14: The schematic view of reactive perforated silencer. 38
Figure 5-15: The picture of perforated tubes a) dh = 2 mm and ϕ = 7.2% staggered array b) dh = 4 mm and ϕ = 7.2% straight array c) dh = 4 mm and ϕ = 28.8% staggered array d) dh = 4 mm and ϕ = 28.8% straight array 39
Figure 5-16: Transmission Loss of reactive perforated tube with dh= 2 mm and ϕ = 7.2% 40
Figure 5-17: Transmission Loss of reactive perforated tube with dh= 4 mm and ϕ = 7.2% 41
Figure 5-18: Transmission Loss of reactive perforated tube with dh= 4 mm and ϕ = 28.8% (Staggered array) 41
Figure 5-19: Transmission Loss of reactive perforated tube with dh= 4 mm and ϕ = 28.8% (Straight array) 42
Figure 5-20: Transmission Loss of reactive perforated silencers (Experiment) 42
Figure 5-21: Stainless steel perforated tube with dh= 4 mm and ϕ = 28.8% 43
Figure 5-22: Transmission loss of stainless steel tube and third prototype sample with dh= 4 mm and ϕ = 28.8% 43
Figure 5-23: The schematic view of dissipative perforated silencer. 44
Figure 5-24: Transmission Loss of dissipative perforated silencer (dh= 4 mm and ϕ = 28.8%) 45
Figure 5-25: Transmission Loss of dissipative perforated silencers (BEM) 45
Figure 5-26: The schematic view of hybrid silencer 46
Figure 5-27: The picture of the hybrid silencer 46
Figure 5-28: BEM model of the hybrid silencer 47

Figure 5-29: Transmission Loss of Hybrid Silencer with 100 mm length of QWT (dh= 4 mm and ϕ = 28.8%) 48
Figure 5-30: Transmission Loss of Hybrid Silencer with 120 mm length of QWT (dh= 4 mm and ϕ = 28.8%) 48
Figure 5-31: Transmission Loss of Hybrid Silencer with 140 mm length of QWT (dh= 4 mm and ϕ = 28.8%) 49
Figure 5-32: Transmission Loss of Hybrid Silencers (Experiment) 49
Figure 5-33: Transmission Loss comparison of dissipative perforated tube, hybrid silencer and QWT (QWT length = 100 mm) 50
Figure 5-34: Transmission Loss comparison of dissipative perforated tube, hybrid silencer and QWT (QWT length = 120 mm) 50
Figure 5-35: Transmission Loss comparison of dissipative perforated tube, hybrid silencer and QWT (QWT length = 140 mm) 51

LIST OF TABLES

TABLES

Table 3-1: $\lambda m, n$, zeros of derivatives of the Bessel Function 8
Table 4-1: Two sets boundary condition of muffler.....21
Table 5-1: Recommended maximum frequency based on microphone diameters.....32

LIST OF ABBREVIATIONS

BEM	Boundary Element Method
QWT	Quarter Wave Tube
FEM	Finite Element Method
TL	Transmission Loss
IL	Insertion Loss
CAD	Computer Aided Design

NOMENCLATURE

L	length of the silencer
d_1	diameter of internal tube
d_2	diameter of external chamber
c_0	speed of sound in the air
D	diameter of the tube
m, n	mode shape numbers
$\lambda_{m,n}$	the roots of Bessel function
f_c	cut-off frequency
ρ_0	air density
p_1	acoustic pressure in domain 1
p_2	acoustic pressure in domain 2
u_1	particle velocity in domain 1
u_2	particle velocity in domain 2
ρ_1	density in domain 1
ρ_2	density in domain 2
V	mean flow velocity
w	the acoustical particle velocity
ξ_p	the acoustical impedance of the perforation
p	pressure of plane wave
ρ	density of plane wave
$\tilde{c}$	complex speed of sound in the absorbing material
d_h	hole diameter of perforation
k_0	wavenumber
$\tilde{k}$	complex wavenumber in the absorbing material
$\tilde{\rho}$	effective density of the absorbing material
M	Mach number
$[\phi]$	the modal matrix
λ_n	the eigenvalues
R_1	the specific flow resistance per unit thickness
Δp	pressure difference
v	the face velocity
t	time period
S	the sample area
h	the porosity of the absorbing material
ρ_A	the filling density of the absorbing material
ρ_M	the material density of the fiber
Z_0	characteristic impedance of the air
$\tilde{Z}$	complex characteristic impedance of the absorbing material
Z_h	the specific acoustic impedance
u_h	the particle velocity through the hole
R_h	the specific resistance of the hole
l_{eff}	the effectice length of the hole
$\mathrm{t_w}$	wall thickness
d_h	diameter of the hole
α	correction coefficient
ξ_h	the non-dimensional acoustic impedance of a single hole
ϕ	porosity
n_h	number of the hole

A_h	area of the hole
A_1	area of the perforated duct
R	the non-dimensional resistance
ξ_p	impedance of perforation including effect of the filling material
S_t	side branch area
S_d	tube cross sectional area
l_e	effective length of the side branch
λ_q	fundamental resonance wavelength of the QWT
f_q	fundamental resonance frequency of QWT
p_I	incident pressure of the duct
p_T	transmitted pressure of the duct
p_R	reflected pressure of the duct
p_s	sound pressure at the entrance of side branch
v_s	sound velocity at the entrance of side branch
Z_s	the impedance of side branch
A_1	incident wave at the source part of impedance tube
B_1	reflecting wave at the source part of impedance tube
A_2	incident wave at the receive part of impedance tube
B_2	reflecting wave at the receive part of impedance tube
P_1	pressure at measurement point 1
P_2	pressure at measurement point 2
P_3	pressure at measurement point 3
P_4	pressure at measurement point 4
P_1^*	the conjugate of P_1
S_{11}	auto-spectrum of measured data at first microphone
S_{12}	cross-spectrum between measured data at first and second microphone
S_{13}	cross-spectrum between measured data at first and third microphone
S_{14}	cross-spectrum between measured data at first and fourth microphone
A_{1o}	incident wave at the source part of impedance tube with open ended load
A_{2o}	incident wave at the recieve part of impedance tube with open ended load
B_{1o}	reflecting wave at the source part of impedance tube with open ended load
B_{2o}	reflecting wave at the recieve part of impedance tube with open ended load
A_{1c}	incident wave at the source part of impedance tube with close ended load
A_{2c}	incident wave at the recieve part of impedance tube with close ended load
B_{1c}	reflecting wave at the source part of impedance tube with close ended load
B_{2c}	reflecting wave at the recieve part of impedance tube with close ended load
f_l	lower working frequency
f_u	upper working frequency
s	spacing between the microphones
T	temperature
p_a	atmospheric pressure
T_0	referance temperature
H_{12}^{I}	measuremnt of transfer function in Configuration I
H_{12}^{II}	measuremnt of transfer function in Configuration II
H_c	calibration factor
S_{11}^{I}	auto-spectrum of microphone 1 in Configuration I
S_{12}^{I}	cross-spectrum between microphone 1 and 2 in Configuration I
S_{11}^{II}	auto-spectrum of microphone 1 in Configuration II
S_{12}^{II}	cross-spectrum between microphone 1 and 2 in Configuration II
$\widehat{H}_{12}$	uncorrected transfer function

CHAPTER 1

INTRODUCTION

1.1 Background

The main difference between the harsh environment electronic equipment and commercial electronics is the environment in which they perform. Operational temperature ranges of harsh environment microelectronics are higher than those of electronics of domestic appliances. Several heat transfer mechanisms are used to remove heat from the chip to the surrounding environment through three basic heat transfer methods, namely, conduction, convection and radiation. [1]

In military industry, thermal management applicability depends on some criteria such as cost, ease of use, thermal performance, and reliability [1]. Considering the criteria defining the efficiency of thermal management methods, radiation and convection are the most reliable methods. In addition, these methods have less complexity and lower cost. However, cooling capacity of combined convection and radiation is less than forced air cooling and liquid cooling methods. For decades, as shown in Figure 1-1, forced air cooling method in which an air handling device is used to move the air through the equipment is preferred because it removes more heat from natural convection technique. In essence, liquid cooling may be more efficient than forced air cooling. However, when liquid is used to remove heat from the device, a heat exchanger is required to cool this liquid. Thereby, the cost and weight of liquid cooling increase, while the reliability of the method decreases.

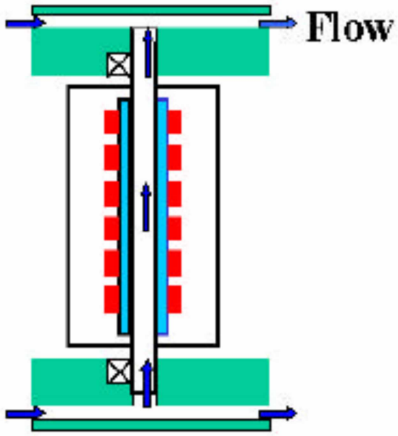

Figure 1-1: Forced air cooling schemes for military electronics

Determining the thermal management method as forced air cooling, the fan noise has to be considered because of comfort of the operator and confidence when using the equipment at rural area. Fan rotation is the main source of noise emitted by a fan. The fan produces a pure tone if the fan is periodically disturbed by inflow acts or interaction between the fan blades and a stationary obstacle

such as vanes or mounting struts. The product of the fan rotational speed and the number of blades gives the lowest frequency of the pure tone known as blade passing frequency. [2]

The rotation of fan generates broadband noise, including particularly strong pure tone at low frequencies. In such cases, dissipative silencers overcome the problem of broadband noise. In addition to this, dissipative silencer can be enhanced to attenuate the pure tone noise at low frequencies by reactive acoustic resonators such as quarter wave tube (QWT) tuned to the frequency of the pure tone.

This study arises from the need for further reduction of noise emitted a rotating machinery at a certain frequency, i.e. fan. The air handling device is used in forced air cooling for thermal management of electronic equipment to be on the safe side of the noise limits for military equipment. Thus, the aim of this study is an acoustical evaluation of dissipative silencer enhanced with QWT resonator that provides the reduction of noise at specific frequencies. It is projected that both tonal components and broadband characteristics of fan noise can be effectively controlled. The study deals with the behavior of the silencer investigated analytically, numerically and experimentally. Firstly, transmission losses of simple expansion chamber and reactive perforated silencer are determined by analytical and computational approach in order to compare the result of experiments. Secondly, experimental and numerical solutions are used to find the transmission loss of the dissipative perforated silencer. Finally, the enhancement of QWT resonator to dissipative silencer is investigated by predicting the transmission loss of the hybrid silencer by numerically and experimentally.

1.2 Thesis Organization

The thesis is organized in six chapters. Following the introduction part, studies about defining the acoustic properties of dissipative silencer are presented in Chapter 2. Analytical formulations for the transmission loss of a silencer that can be a simple expansion chamber, reactive perforated silencer and dissipative perforated silencer is described in Chapter 3. Acoustical properties of absorbing materials and effects of perforation to determine transmission loss are described in Chapter 3. Moreover, acoustic evaluation of QWT resonator is also stated in this chapter. Chapter 4 includes requirements for a computational model of the silencer with perforation and sound absorbing material. Two experimental schemes established for all silencers covered before and characteristic impedance and wavenumber of absorbing material are presented in Chapter 5. In Chapter 5, the comparison of transmission losses of silencers with each other are also examined. Finally, Chapter 6 presents a summary and conclusions of the study with suggestions for future work.

CHAPTER 2

LITERATURE SURVEY

In this chapter relevant previous researches about the design of dissipative silencer and hybrid silencer are overviewed. The literature survey consists of three main parts, namely,analytical, numerical and experimental methods, to predict the transmission loss of a silencer.

2.1 Analytical Methods

Attenuation characteristics of various acoustic silencers have been investigated. Igarashi et al. [3] used an equivalent electrical network (Figure 2-1) to represent the acoustic elements, such as cavities, resonators, internal tube type cavities and cavities with absorbing material. Four terminal matrices are presented to symbolize each acoustic element. Transmission loss is calculated from product of these four pole matrices.

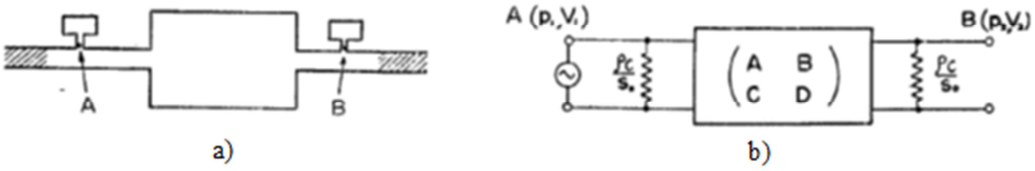

Figure 2-1: The schematic view of a) expansion chamber (cavity) b) equivalent circuit of a cavity element. [3]

Low frequency resonator, providing attenuation between 50-4000 Hz, is usually used in automotive industries. However, it has irregular large shapes and is connected to the exhaust with single large diameter tube or neck. On the other hand, high frequency resonator has a concentric-tube, having perforation elements on entire lengths, and rigid shell around the tube. The coupling of the tube and the cavity is provided by perforation elements. Simple theory used to predict the transmission loss of the low-frequency resonator is not valid for the high frequency case because of the energy losses at the holes. Sullivan and Crocker [4] provide an empirical transfer impedance formula for perforation elements in the high frequency resonator. The mathematical model is obtained for the case of zero mean flow and experimental observations agree with the transfer matrix method.

Sullivan [5] presents a theory for modeling one-dimensional perforated muffler elements by using segmentation method. The muffler is divided into several segments each of which is presented by a transmission matrix. The product of these transmission matrices provides the four-pole parameters for through flow, cross flow and reverse flow. This method differs from others with mean flow, avoiding high dimensionality and not requiring matrix inversion. The transmission loss is computed from the product of 4 x4 complex matrices for two-duct configurations. Hence, the

calculation times are less than methods such as finite element that requires high speed computational power and storage capacities.

A one-dimensional distributed model of a uniform perforate impedance is presented by Jayaraman and Yam [6]. In this study, decoupling the two differential equations with the assumption of equal mean flow in multi-duct configuration describes one-dimensional acoustic wave propagation.

In several studies, when prediction of the sound attenuation in a lined circular flow duct, models have not counted effect of internal mean flow velocities in the porous liner. Cummings and Chang [7] establish a study with an objective to present the effect of the mean flow within the liner on the attenuating properties of the absorbent and to present theoretical model for determining these effects. The real part of the flow resistivity of the absorptive material is affected by the internal mean flow within the liner and the attenuation properties are improved or detracted.

Several studies have been examined to determine transmission loss with one-dimensional wave propagation having inaccuracies at high frequencies. Selamet and Radavich [8] present a study to investigate in detail the effect of the circular concentric expansion chamber geometry on the transmission loss for one-dimensional versus multi-dimensional propagation. The transmission loss is determined by two-dimensional analytical approach, three-dimensional numerical method and these methods are verified by experimental results. It is reported that, although multi-dimensional waves exist at all frequencies, multi-dimensional effects begin to dominate at higher frequencies.

Mufflers are widely used in various industries to attenuate the noise levels radiated outside of the atmosphere. High performance and reliable methods are needed to design a muffler. BEM/FEM are appropriate methods and commonly used to model the complex shape mufflers. However, these are expensive and time-consuming for preliminary design evaluation. Gerges and Jordan [9] summarize the fundamentals of the transfer matrix method and apply the methods different muffler configuration to predict the transmission loss without needing high speed computational power and storage capacity. Experimental measurements of these different muffler designs are carried to compare the results with numerical predictions. Comparison of the results shows that plane wave based models can offer fast initial preliminary solutions for muffler designers.

2.2 Numerical Methods

In the past studies on evaluation of transmission loss for a resonator with BEM, the effect of the mean flow on the performance of the resonator is not included. However, Wang et al. [10] introduce a study that presents a boundary element method approach for a straight-through resonator with mean flow. In their study, both convection effects and change of acoustic impedance are considered as an influence of mean flows. The mean flow effects on performance of long and short resonators are presented. Further, acoustic performance of a resonator with mean flow is influenced by porosity, tube thickness and drilling hole diameter. These parameters are also investigated in this study.

When the BEM is used to model a muffler, transmission loss is determined by a four-pole method or three-point method. Three-point method requires less time than four-pole method because only transmission loss is produced by three-point method while four-pole method gives both transmission loss and other parameters of the muffler by computing two transfer matrices. Wu et al. [11] improve a new four-pole method to evaluate transmission loss of a muffler by computing just one BEM matrix at each frequency. So, the improved method is as fast as the three-point method because it solves one BEM matrix. It also produces other important parameters of mufflers. In this study, transmission loss determined by the improved method is compared with that found from experiments.

Young and Croker [12] present one of the first studies about determining transmission loss in complicated shaped mufflers with FEM. They develop a new numerical technique based on FEM to predict the transmission loss of the expansion chamber. The transmission loss is found by forming

four-terminal transmission network in which four-pole constants are calculated with FEM. In this study, the method is applied to a simple expansion chamber such that the results can be compared with those of theoretical methods. When the results are compared with the plane - wave solution, it is discovered there is a good agreement between finite element approach and analytical approach. Young and Croker [13] also present a study about predicting the transmission loss characteristics of flow-reversing muffler chambers by using numerical approach based on FEM. They compare the predicted transmission loss value with experimental results of various chambers that have different inlet-outlet configurations. As an outcome of this study, the transmission loss characteristics of flow-reversing muffler chambers are found to be dependent on the inlet-outlet configurations.

2.3 Experimental Methods

Prediction of transmission loss from an experimental setup is surely different from analytical calculations. Recent studies present some evaluation methods to determine the transmission loss from measured data.

The standard two-microphone random excitation method including the transmission loss calculation is described by Chung and Blaser [14]. Incident and reflected components of a broadband stationary random signal are decomposed using simple transfer function between the two upstream microphones to determine the complex reflection coefficient from acoustical properties such as acoustic impedance, the transmission loss and the sound absorption coefficient. Furthermore, experimental results are compared with theoretical predictions and the study presents these results agree with each other.

Seybert and Ross [15] present a study about an experimental method to predict the acoustic properties in a tube considering mean flow. In the study, two wall-mounted microphones are used to measure the white noise generated by a speaker. Auto and cross spectrum of the signal measured by the microphones are calculated to show incident and reflected waves, and phase angles between them. So, acoustic impedance and absorption coefficient are expressed with auto and cross spectrum of the incident and reflected wave. In addition to this, a third microphone is used to measure transmission loss of a test specimen.

The transmission loss of a muffler is determined by experimental methods The most common ones are the two load method and two source method shown in Figure 2-2 and Figure 2-3. Tao and Seybert [16] present a study including the comparison of these two common methods. In both cases, measured transmission loss is compared with predicted value obtained by boundary element method. The main difference between these methods is expressed as the two load method is easier to measure transmission loss while both transmission loss and four pole parameters of a muffler can be measured by the two-source method.

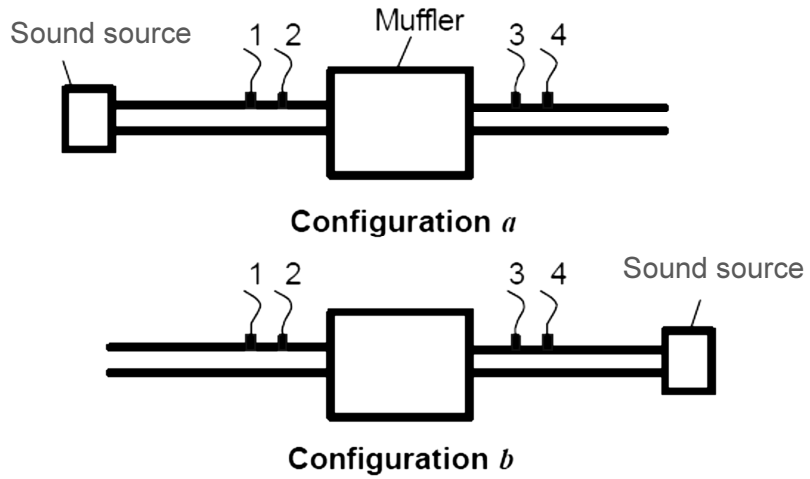

Figure 2-2: Test setup for Two Source Method [16]

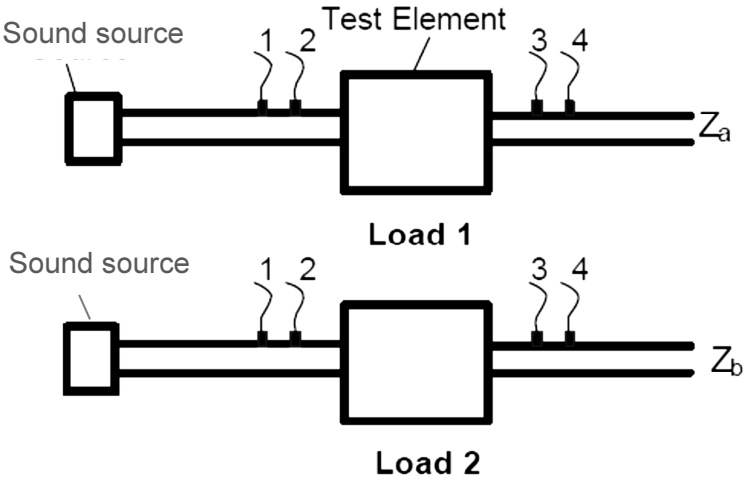

Figure 2-3: Test setup for Two Load Method [16]

The classical method of transmission loss measurement is two room method. In this method the test specimen is placed in the opening between anechoic and a reverberant room. Two microphones located in each room are used to measure the sound generated in the reverberant room. This reliable method is well defined in previous studies, but it is very expensive. In recent years, the number of various transmission loss measurement methods are studied and two-load method is one of them. The comparison of two-load and reliable two-room method of transmission loss measurements is studied by Yousefzadeh et al. [17] Besides different tube termination conditions are considered and the results of these different measurements are compared with those two room method.

CHAPTER 3

THEORETICAL MODELS

This chapter presents to predict the transmission loss of dissipative with one dimensional analytical approach and insertion loss of dissipative and hybrid silencer. Acoustic properties of absorbing material and perforation are required to determine the transmission loss of a dissipative perforated silencer. In this chapter some expressions are introduced for defining the impedance of both filling material and perforation.

3.1 Acoustic Performance of Silencer

A one-dimensional analytical approach is presented next to determine the transmission loss of the dissipative silencer of length L, main duct diameter d_1 and outer chamber diameter d_2. The schematic presentation of dissipative silencer and the properties are shown in Figure 3-1.

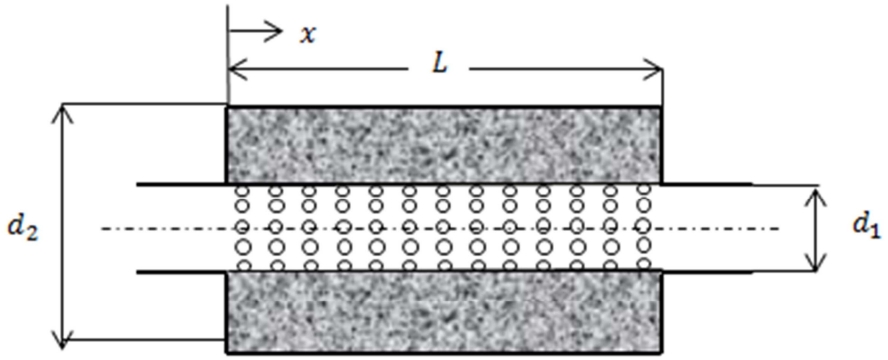

Figure 3-1: The schematic of a perforated dissipative single-pass straight silencer.

The sound wave propagation of a duct is simple and one dimensional over a frequency range whose corresponding wavelength is longer than the transverse dimensions of the duct. In fact, only plane wave can propagate below a certain frequency that is dependent on the transverse dimension and shape of the duct. Plane wave propagation provides that the sound field in the duct becomes one-dimensional. Besides, higher order modes appear when the wavelength decreases and crosses the dimensions of the duct. As the wavelength becomes the same order of the transverse dimensions, cut-off frequencies, f_c, appear in the sound field and are expressed as [18]

$$f_c = \lambda_{m,n} \frac{c_0}{\pi D} \tag{3-1}$$

where $\lambda_{m,n}$ is the roots of Bessel function described in Eriksson study [18]. The mode shapes and values of the roots are shown in Figure 3-2. The roots of Bessel function are also tabulated in Table 3-1.

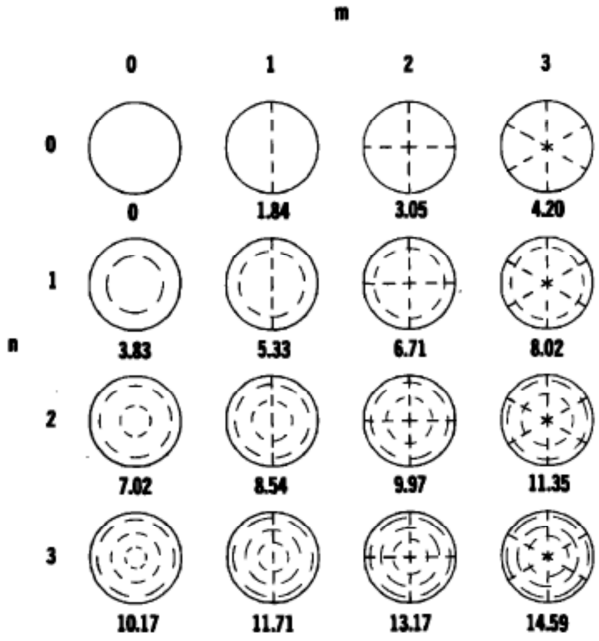

Figure 3-2: The mode shapes and zeros of derivatives of the Bessel Function [18]

Table 3-1: $\lambda_{m,n}$, zeros of derivatives of the Bessel Function [18]

	m			
n	**0**	**1**	**2**	**3**
0	0	1.84	3.05	4.2
1	3.83	5.33	6.71	8.02
2	7.02	8.54	9.97	11.35
3	10.17	11.71	13.17	14.59

Wyerman [19] indicates existing three distinct types of modes after analyzing the radial mode shapes. Plane wave without radial or circumferential dependence is the first mode shape. Secondly, higher order modes of $m = 0$ have radial dependence, but there is no circumferential dependence. Final modes are higher order modes of $m = 1,2,3$ ... that have both radial and circumferential dependences. Final modes having circumferential dependence is called spinning or spiral modes.

Besides, Fan et al. [20] present other resonance frequencies wavelengths of which are distributed around the circumference of the cylinder. The wavelengths of corresponding resonance frequencies are presented by an integer number n as following formula;

$$\lambda_n = \frac{2\pi r}{n} \tag{3-2}$$

where λ_n is the wavelength of the resonance frequency and r is the radius of a cylinder.

The plane wave propagation in the main duct and the absorbent material is presented by Wang [21] by obtaining a transfer matrix between the inlet and outlet of the duct. The continuity and momentum equations are expressed as;

$$\rho_0 \frac{\partial u_1}{\partial x} + V \frac{\partial \rho_1}{\partial x} + \frac{4}{d_1}\rho_0 w + \frac{\partial \rho_1}{\partial t} = 0 \tag{3-3}$$

$$\rho_0 \left(\frac{\partial}{\partial t} + V \frac{\partial}{\partial x}\right) u_1 + \frac{\partial p_1}{\partial x} = 0 \tag{3-4}$$

for the center tube, and

$$\tilde{\rho} \frac{\partial u_2}{\partial x} - \frac{4 d_1}{{d_2}^2 - {d_1}^2} \tilde{\rho} w + \frac{\partial \rho_2}{\partial t} = 0 \tag{3-5}$$

$$\tilde{\rho} \frac{\partial u_2}{\partial t} + \frac{\partial p_2}{\partial x} = 0 \tag{3-6}$$

for the outer chamber, where u_1, u_2, ρ_1, ρ_2, p_1, p_2 denote the axial particle velocity, density and pressure; while ρ_0, V, and w represent the mean density, mean flow velocity and the acoustic particle velocity through the perforation, respectively. The acoustic impedance of the perforation and the relation of pressure and density of plane wave are presented as;

$$\xi_p = \frac{\Delta p}{w \rho_0 c_0} \tag{3-7}$$

$$p = \rho {c_0}^2 \tag{3-8}$$

Using with Eq. (3-3) – (3-6) and by eliminating velocity and density, new expressions are obtained;

$$\frac{d^2 p_1}{dx^2} + a_1 \frac{dp_1}{dx} + a_2 p_1 + a_3 \frac{dp_2}{dx} + a_4 p_2 = 0 \tag{3-9}$$

$$\frac{d^2 p_2}{dx^2} + a_5 p_2 + a_6 p_1 = 0 \tag{3-10}$$

where

$$a_1 = -\frac{2ik_0 M + \frac{4}{d_1}\frac{M}{\xi_p}}{1 - M^2} \qquad a_2 = \frac{{k_0}^2 - \frac{4}{d_1}\frac{ik_0}{\xi_p}}{1 - M^2}$$

$$a_3 = \frac{\frac{4}{d_1}\frac{M}{\xi_p}}{1-M^2} \qquad a_4 = \frac{\frac{4}{d_1}\frac{ik_0}{\xi_p}}{1-M^2}$$

$$a_5 = \tilde{k}^2 - \frac{4d_1}{{d_2}^2 - {d_1}^2}\frac{\tilde{\rho}}{\rho_0}\frac{ik_0}{\xi_p} \qquad a_6 = \frac{4d_1}{{d_2}^2 - {d_1}^2}\frac{\tilde{\rho}}{\rho_0}\frac{ik_0}{\xi_p}$$

$$M = \frac{V}{c_0} \qquad k_0 = \frac{\omega}{c_0} \qquad \tilde{k} = \frac{\omega}{\tilde{c}}$$

The second order equations may be rearranged as four equations,

$$\begin{Bmatrix} {p_1}' \\ \left(\frac{dp_1}{dx}\right)' \\ {p_2}' \\ \left(\frac{dp_2}{dx}\right)' \end{Bmatrix} = \begin{bmatrix} 0 & 1 & 0 & 0 \\ -a_2 & -a_1 & -a_4 & -a_3 \\ 0 & 0 & 0 & 1 \\ -a_6 & 0 & -a_5 & 0 \end{bmatrix} \begin{Bmatrix} p_1 \\ \frac{dp_1}{dx} \\ p_2 \\ \frac{dp_2}{dx} \end{Bmatrix} \tag{3-11}$$

Using the linearized momentum equation and Eq. (3-8) into Eq. (3-11), the expression become as,

$$\begin{Bmatrix} {p_1}' \\ \rho_0 c_0 {u_1}' \\ {p_2}' \\ \tilde{\rho}\tilde{c}{u_2}' \end{Bmatrix} = \begin{bmatrix} 0 & -ik_0 & 0 & 0 \\ \frac{1}{ik_0}a_2 & \frac{1}{ik_0}a_1 & \frac{1}{ik_0}a_4 & \frac{1}{ik_0}a_3 \\ 0 & 0 & 0 & -i\tilde{k} \\ \frac{1}{i\tilde{k}}a_6 & 0 & \frac{1}{i\tilde{k}}a_5 & 0 \end{bmatrix} \begin{Bmatrix} p_1 \\ \rho_0 c_0 u_1 \\ p_2 \\ \tilde{\rho}\tilde{c}u_2 \end{Bmatrix} \tag{3-12}$$

$$\begin{Bmatrix} {p_1}' \\ \rho_0 c_0 {u_1}' \\ {p_2}' \\ \tilde{\rho}\tilde{c}{u_2}' \end{Bmatrix} = [TA] \begin{Bmatrix} p_1 \\ \rho_0 c_0 u_1 \\ p_2 \\ \tilde{\rho}\tilde{c}u_2 \end{Bmatrix} \tag{3-13}$$

The eigenvalues and eigenvectors of the solution are expressed as;

$$\begin{Bmatrix} p_1(x) \\ \rho_0 c_0 u_1(x) \\ p_2(x) \\ \tilde{\rho}\tilde{c}u_2(x) \end{Bmatrix} = [\phi] \begin{Bmatrix} c_1 e^{\lambda_1 x} \\ c_2 e^{\lambda_2 x} \\ c_3 e^{\lambda_3 x} \\ c_4 e^{\lambda_4 x} \end{Bmatrix} \tag{3-14}$$

$[\phi]$ is the modal matrix whose columns are the eigenvectors. The eigenvalues are expressed as λ_n and c_n is the arbitrary constant.

$$\Psi_{1i} = \phi_{1i} e^{\lambda_1 x}$$

$$\Psi_{2i} = \phi_{2i} e^{\lambda_2 x}$$

$$\Psi_{3i} = \phi_{3i} e^{\lambda_3 x}$$

$$\Psi_{4i} = \phi_{4i} e^{\lambda_4 x}$$

After elements of $[\Psi]$ modal matrix is defined, Eq.(3-14) can be rearranged as;

$$\begin{Bmatrix} p_1(x) \\ \rho_0 c_0 u_1(x) \\ p_2(x) \\ \tilde{\rho}\tilde{c} u_2(x) \end{Bmatrix} = [\Psi(x)] \begin{Bmatrix} c_1 \\ c_2 \\ c_3 \\ c_4 \end{Bmatrix} \tag{3-15}$$

Therefore, these expressions lead to relationship between acoustic pressure and particle velocity at inlet and outlet as,

$$\begin{Bmatrix} p_1(0) \\ \rho c u_1(0) \\ p_2(0) \\ \rho c u_2(0) \end{Bmatrix} = [TB] \begin{Bmatrix} p_1(L) \\ \rho c u_1(L) \\ p_2(L) \\ \rho c u_2(L) \end{Bmatrix} \tag{3-16}$$

where

$$[TB] = [\Psi(0)][\Psi(\mathrm{L})]^{-1} \tag{3-17}$$

Two boundary conditions for the outer chamber are required to determine the transmission loss of the dissipative silencer. The impedance of the expansion chamber at $x = 0$ and $x = L$ are expressed as,

$$\tilde{Z}(0) = -\frac{p_2(0)}{u_2(0)} = -i\tilde{\rho}\tilde{c} \tag{3-18}$$

$$\tilde{Z}(L) = -\frac{p_2(L)}{u_2(L)} = -i\tilde{\rho}\tilde{c} \tag{3-19}$$

Finally, in order to derive the transfer matrix between the inlet and the outlet of the center tube $p_2(0)$, $u_2(0)$, $p_2(L)$ and $u_2(L)$ should be eliminated from Eq. (3-16) and the expression is rearranged as;

$$\begin{Bmatrix} p_1(0) \\ \rho c u_1(0) \end{Bmatrix} = \begin{bmatrix} T_{11} & T_{12} \\ T_{21} & T_{22} \end{bmatrix} \begin{Bmatrix} p_1(L) \\ \rho c u_1(L) \end{Bmatrix} \tag{3-20}$$

where

$$T_{11} = TB_{11} - \frac{TB_{13}TB_{41}}{TB_{43}} \tag{3-21}$$

$$T_{12} = TB_{12} - \frac{TB_{13}TB_{42}}{TB_{43}} \tag{3-22}$$

$$T_{21} = TB_{21} - \frac{TB_{23}TB_{41}}{TB_{43}} \tag{3-23}$$

$$T_{22} = TB_{22} - \frac{TB_{23}TB_{42}}{TB_{43}} \tag{3-24}$$

The transfer matrix is formed and four pole parameters are evaluated, assuming the constant cross sectional area of the main duct transmission loss of the dissipative silencer can be obtained as;

$$TL = 20\log_{10}\left(\frac{|T_{11}+T_{12}+T_{21}+T_{22}|}{2}\right) \tag{3-25}$$

3.2 Acoustical Properties of Absorbing Material

Sound absorbing materials are available in many forms such as glass, mineral or organic fibers, mats, boards or foams. As they have open pores dimension of which is smaller than the wavelength of the sound, they can be assumed as a lossy homogeneous medium. [22]

In order to determine the transmission loss of a silencer, physical and acoustical properties of an absorbing material have to be known. In this section properties of glass fiber that is selected as an absorbing material in this study are examined.

3.2.1 Physical Properties of Absorbing Material

Flow resistivity is the most important property of the fibrous material. Beranek [19] defines the specific flow resistance per unit thickness as;

$$R_1 = -\frac{1}{v}\frac{\Delta p}{\Delta x} = -\frac{tS}{V}\frac{\Delta p}{\Delta x} \qquad \text{N·s/m}^4 \text{ (mks rayls/m)} \tag{3-26}$$

where Δp is the pressure difference across the homogeneous layer thickness of which is Δx, v is face velocity of the flow through the material, V is the volume of air passing through the sample during the time period t, S is the sample area.

Another important physical property of the absorbing material is porosity defined as the ratio of the pore volume to total volume. Porosity can be calculated from an expression which is defined by Beranek [22].

$$h = 1 - \frac{\rho_A}{\rho_M} \tag{3-27}$$

where h is the porosity of the absorbing material and it is calculated using filling density ρ_A and the material density of the fiber ρ_M.

3.2.2 Acoustical Characterization of Absorbing Material

The characteristic of the fibrous sound-absorbing material is expressed in terms of complex characteristic impedance and wavenumber. The real part of the wavenumber is attenuation constant and it is easily measured with a probe tube microphone. Measuring the change of phase with distance provide to determine the imaginary part of the wavelength. Similarly, the characteristic impedance is also found by an impedance tube experiment. Delany and Bazley [23] define empirical expressions for both complex characteristic impedance and wavelength. The expressions are formed and combined with the results obtained from different techniques. When presenting the expression they use a non - dimensional form as;

$$\frac{\tilde{Z}}{Z_0} = \left[1 + 0.0511\left(\frac{f}{R_1}\right)^{-0.75}\right] + i\left[-0.0768\left(\frac{f}{R_1}\right)^{-0.73}\right] \tag{3-28}$$

$$\frac{\tilde{k}}{k_0} = \left[1 + 0.0858\left(\frac{f}{R_1}\right)^{-0.70}\right] + i\left[-0.1749\left(\frac{f}{R_1}\right)^{-0.59}\right] \tag{3-29}$$

where f denotes frequency, $Z_0 = \rho_0 c_0$ is the characteristic impedance of the air and $k_0 = \frac{2\pi f}{c_0}$ is the wavenumber in air.

3.3 Acoustic Impedance of the Perforation

Perforated silencer composed of main tube and outer chamber, and perforated surface is an interface between these domains. Hence, acoustic impedance of the perforation is essential to characterize acoustic properties of the silencer because perforation contacts acoustic waves in main duct and outer chamber.

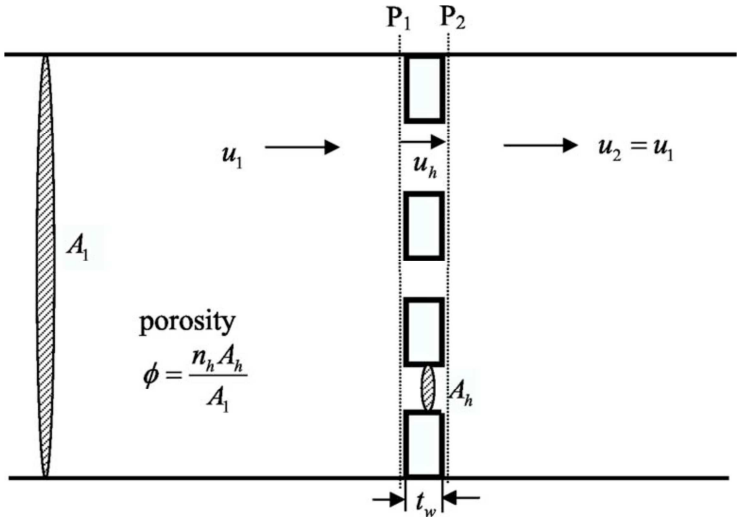

Figure 3-3: Wave propagation through a perforated plate in a duct. [24]

The acoustic impedance of perforated tube is derived from impedance of a hole which composes the perforation. Lee et al. [24] present a study about defining acoustic impedance of a hole

and perforated plate, in this section the derivation of the impedance of perforated tube is examined. The non-dimensional acoustic impedance of a hole is expressed as

$$\xi_h = \frac{Z_h}{\rho_0 c_0} \tag{3-30}$$

where Z_h is the specific acoustic impedance of a single hole and defined as

$$Z_h = \frac{p_1 - p_2}{u_h} \tag{3-31}$$

where $p_1 - p_2$ is the pressure difference across the hole and u_h is the particle velocity through the hole. The specific acoustic impedance can be written as;

$$Z_h = R_h + i\omega\rho_0 l_{eff} = R_h + ik_0 c_0 \rho_0 l_{eff} \tag{3-32}$$

where R_h is the specific resistance of the hole and l_{eff} is the effective length of the hole and can be expressed as;

$$l_{eff} = t_w + \alpha d_h \tag{3-33}$$

where t_w and d_h are the wall thickness and the diameter of the hole located on the perforated plate, respectively. Besides, α is the correction coefficient and depends on geometry of the hole.

Eq. (3-30), the non-dimensional acoustic impedance of a single hole, can be rewritten as;

$$\xi_h = \frac{R_h + ik_0 c_0 \rho_0 (t_w + \alpha d_h)}{\rho_0 c_0} = \frac{R_h}{\rho_0 c_0} + ik_0(t_w + \alpha d_h) \tag{3-34}$$

where $\frac{R_h}{\rho_0 c_0}$ is the non-dimensional resistance and can be called R.

The non-dimensional acoustic impedance of the perforated plate can be expressed as;

$$\xi_p = \frac{p_1 - p_2}{u_1 \rho_0 c_0} \tag{3-35}$$

where u_1 is the particle velocity in the duct and can be associated with u_h as;

$$u_1 = \phi u_h \tag{3-36}$$

where

$$\phi = \frac{n_h A_h}{A_1} \tag{3-37}$$

where number and area of the hole are denoted as n_h and A_h, respectively. A_1 is the area of the perforated duct.

Using Eq. (3-36) into Eq. (3-35), the non-dimensional acoustic impedance of the perforation can be rearranged as;

$$\xi_p = \frac{p_1 - p_2}{\rho_0 c_0 u_h \phi} = \frac{\xi_h}{\phi} = \frac{R + ik_0(t_w + \alpha d_h)}{\phi} \tag{3-38}$$

3.3.1 Acoustic Impedance of Air-Air Interaction

Acoustic impedance of hole and perforated plate is derived previous section. Eq. (3-38) can be used as acoustic impedance of perforation plate between air-air. The resistance *R* and correction coefficient are experimentally determined. In this expression the coefficient factor value is 0.75, because it is associated with the end correction factor. In addition to this *R* is taken 0.006. [4]

The acoustic impedance of perforation between air-air is defined as;

$$\xi_p = \frac{0.006 + ik_0(t_w + 0.75 d_h)}{\phi} \tag{3-39}$$

3.3.2 Acoustic Impedance of Air-Fibrous Interaction

In dissipative silencers fibrous materials are used and placed on one side of the perforated plate. The filling material influences the impedance of the perforation, which alters the overall acoustic characteristics of silencer.

When determining the acoustic characteristic of the dissipative silencer acoustic impedance of absorbing material and perforation can't be separated from each other. Thus, Kirby and Cumming [25] suggest an expression for impedance of perforation including the effect of the filling material.

$$\tilde{\xi}_p = \frac{(\xi_p \phi - i0.425 k_0 d_h + i0.425 \frac{\tilde{Z}}{\rho_0 c_0} \tilde{k} d_h)}{\phi} \tag{3-40}$$

3.4 Acoustic Performance of Quarter Wave Tube [26]

Tube resonator is a useful device to reduce noise of constant frequency, such as constant speed rotational machinery. Length of the QWT resonator is quarter of the wavelength of sound at interest frequency. The name of the resonator is come from length of the tube. The schematic view of the QWT is presented in Figure 3-4.

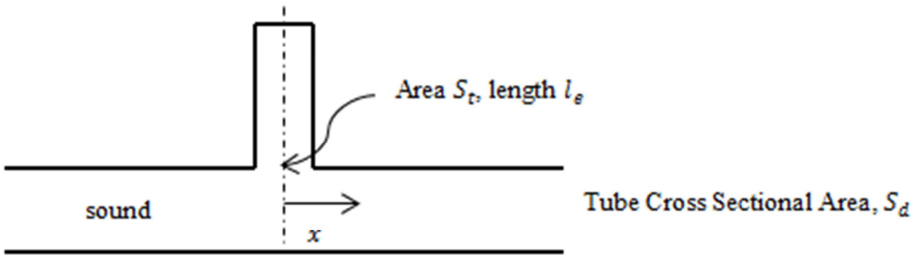

Figure 3-4: The schematic view of QWT resonator

$$l_e = \frac{\lambda_q}{4} \tag{3-41}$$

$$f_q = \frac{c}{\lambda_q} = \frac{c}{4l_e} \tag{3-42}$$

Where l_e is the effective length of the side branch. λ_q and f_q are the fundamental resonance wavelength and frequency of the QWT resonator, respectively.

Transmission loss of the QWT is derived by using the harmonic solution of the wave equation. Because of the dimensions of side branch are small enough, sound propagation is plane wave. Transmission loss is the ratio of incident and transmitted pressure considering plane wave as;

$$TL = 10\log\left|\frac{p_I}{p_T}\right| = 10\log\left|\frac{A_I}{A_T}\right| \tag{3-43}$$

where p_I and p_T are the incident and transmitted pressure of the duct. The sum of the incident pressure, p_I and the reflected pressure, $p_R$is the total sound pressure in the duct. Total pressure and transmitted pressure in the absence of reflected wave are expressed as, respectively;

$$p_{inlet} = A_I e^{j(\omega t - kx)} + A_R e^{j(\omega t + kx + \beta_1)} \tag{3-44}$$

$$p_T = A_T e^{j(\omega t - kx + \beta_2)} \tag{3-45}$$

where β_1 and β_2 are the randomly selected phase angles. The acoustic volume velocities are presented as;

$$v_{inlet} = \frac{S_d}{\rho c}\left[A_I e^{j(\omega t - kx)} + A_R e^{j(\omega t + kx + \beta_1)}\right] \tag{3-46}$$

$$v_T = \frac{S_d A_T}{\rho c} e^{j(\omega t - kx + \beta_2)} \tag{3-47}$$

When the duct axial coordinate x is equal to zero, the sound pressure at the entrance of side branch, p_s, is expressed as;

$$p_s = A_T e^{j(\omega t + \beta_2)} = A_I e^{j(\omega t)} + A_R e^{j(\omega t + \beta_1)} \tag{3-48}$$

At $x = 0$, the incoming velocity from the left is equal to the sum of the entering side branch velocity and the moving velocity to the right, so the entering side branch velocity is written as;

$$v_s = \frac{p_s}{Z_s} = \frac{p_t}{Z_s} \tag{3-49}$$

where the Z_s is the impedance of side branch and is expressed as;

$$Z_s = j\frac{\rho c}{S_t}\frac{1}{\tan(kl_e)} \tag{3-50}$$

Volume velocity at the entering side branch is written as;

$$\frac{S_d}{\rho c}\left[A_I e^{j(\omega t-kx)} - A_R e^{j(\omega t+kx+\beta_1)}\right] = \frac{S_d A_T}{\rho c} e^{j(\omega t-kx+\beta_2)} + A_T e^{j(\omega t+\beta_2)} \quad (3\text{-}51)$$

Simplifying and rearranging as;

$$\frac{2A_I S_d}{\rho c} = A_T e^{j\beta_2}\left(\frac{2S_d}{\rho c} + \frac{1}{Z_s}\right) \quad (3\text{-}52)$$

$$\left|\frac{A_I}{A_T}\right| = \left|1 + \frac{\rho c}{2S_d Z_s}\right| \quad (3\text{-}53)$$

Transmission loss can be expressed as;

$$TL = 20\log\left|1 + \frac{\rho c}{2S_d Z_s}\right| \quad (3\text{-}54)$$

Simplifying and rearranging as;

$$TL = 10\log\left[1 + \left(\frac{S_t}{2S_d}\tan(kl_e)\right)^2\right] \quad (3\text{-}55)$$

CHAPTER 4

NUMERICAL MODELING

BEM is a numerical method to predict acoustic performance of a silencer through solution of linear partial differential equations. It is successfully used in recent years for silencer design in industrial applications. Compared with the traditional analytical calculation, the BEM provides a faster design tool for complex shape silencer or muffler. Furthermore, the BEM is often more efficient than the other computational methods because only the surfaces are required to be modelled.

In this study VNoise BEM solver is used to calculate transmission loss of dissipative perforated silencer numerically. Coupling analysis with multiple fluid properties can be executed with VNoise. The coupling between different fluid domains can be defined. For example, VNoise permits to model of air-fibrous perforated surface in which two different fluid domains are coupled. Furthermore, perforation can be easily defined without the need to geometrically model each hole, while describing simply some properties of perforation such as hole diameter and porosity. In addition to adding the effect of perforation on calculation, acoustical properties of absorbing material can be taken into account by simply assigning complex fluid density and speed of sound which are calculated by the software with some empirical expressions.

4.1 Acoustic Properties of Perforation in VNoise

There are two methods to model the perforation in VNoise; one is detailed description of the perforation geometry with holes, other is using of semi-empirical calculation with global parameters of the perforated surface. The first method provides the best accuracy, but it prevents to select correct element size which is recommended at least 6 linear elements per wavelength corresponding to the highest frequency of interest. Therefore, very refined discretization is needed to define the pressure distribution around the holes, which costs computational time and leads to use second method. The average behavior of the perforated surface is described rather than describing the each point on the perforated surface with the semi-empirical approach. In this approach VNoise calculates the acoustic impedance of the perforated surface with Eq. (3-39) that is derived in previous chapter by using imported properties of perforation such as hole diameter and porosity.

$$\xi_p = \frac{0.006+ik_0(t_w+0.75d_h)}{\phi} \tag{3-39}$$

Although the semi-empirical method has a great advantage not requiring to geometrically model all holes and it saves time, its main disadvantage is about the accuracy in the analysis. However, as shown in Figure 4-1 transmission loss found by using semi-empirical approach well agrees with that measured by experimentally [24].

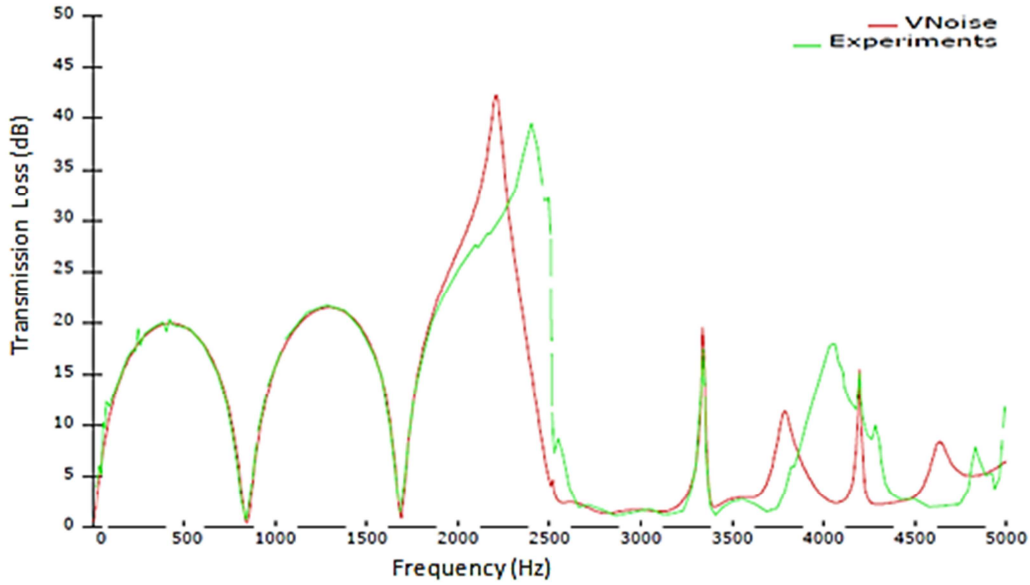

Figure 4-1: Transmission loss of a muffler with porosity 0.098, hole diameter 0.003175 and number holes 276 [24]

4.2 Acoustical Properties of Absorbing Material in VNoise

When determining transmission loss of a dissipative silencer, a new domain has to be defined for absorbing material including complex speed of sound and complex density. VNoise use semi-empirical formulation to find impedance of the material with inserted resistivity. To illustrate, te calculation of complex speed of sound and complex density of glass fiber Eq. (3-28) and Eq. (3-29) are used [23].

$$\frac{\tilde{Z}}{Z_0} = \left[1 + 0.0511\left(\frac{f}{R_1}\right)^{-0.75}\right] + i\left[-0.0768\left(\frac{f}{R_1}\right)^{-0.73}\right] \tag{3.28}$$

$$\frac{\tilde{k}}{k_0} = \left[1 + 0.0858\left(\frac{f}{R_1}\right)^{-0.70}\right] + i\left[-0.1749\left(\frac{f}{R_1}\right)^{-0.59}\right] \tag{3.29}$$

A test setup described in Sec. 5.2 is used to obtain characteristic impedance and complex wavenumber of filling material in the absence of mean flow. In this study filling material with unknown acoustic properties is used in dissipative silencer, so the characteristic impedance and wavenumber measurements are performed to defining the absorbing material in VNoise.

4.3 Evaluation of Transmission Loss and Insertion Loss in VNoise

BEM module is generally used for analysis of muffler and ducts in VNoise. Performance of a muffler can be evaluated by determining the performance indexes transmission loss (TL) or insertion loss (IL). VNoise use some expressions to find these indexes, which is presented in this section. Two waves exist in a generic duct or muffler which is shown in Figure 4-2, one wave called p_1^+ is entering

the muffler and the other called p_1^- is travelling in the opposite direction. Similarly, at the outlet section, there are two waves travelling in opposite directions of each other.

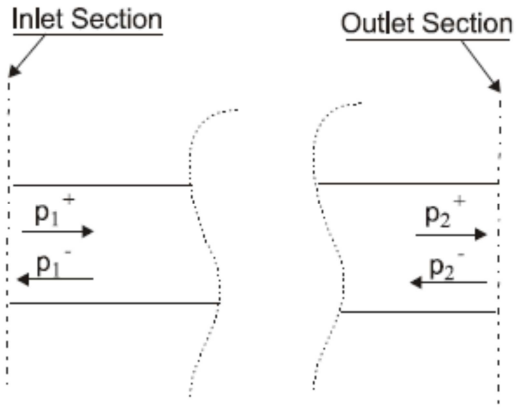

Figure 4-2: Schematic representation of a generic duct or muffler

The velocity and total pressure at the inlet and the outlet can be expressed as;

$$p_1 = p_1^+ + p_1^- \tag{4-1}$$

$$p_2 = p_2^+ + p_2^- \tag{4-2}$$

$$V_1 = \frac{(p_1^+ + p_1^-)}{\rho c} \tag{4-3}$$

$$V_2 = \frac{(p_2^+ + p_2^-)}{\rho c} \tag{4-4}$$

TL and IL evaluation is based on four pole parameter transfer matrix method. These parameters can be easily computed by BEM analysis requiring two sets of boundary condition tabulated in Table 4-1.

Table 4-1: Two sets boundary condition of muffler

Set	Boundary condition at inlet	Boundary condition at outlet
1	Imposed velocity v=1	Imposed velocity v=0
2	Imposed velocity v=1	Imposed pressure p=0

The four pole parameters are complex number and depend on frequency. Computation of the these parameter is expressed as;

$$A = \frac{p_1}{p_2} \qquad \text{from set 1} \tag{4-5}$$

$$C = \frac{v_1}{p_2} \qquad \text{from set 1} \tag{4-6}$$

$$B = \frac{p_1}{v_2} \qquad \text{from set 2} \tag{4-7}$$

$$D = \frac{v_1}{v_2} \qquad \text{from set 2} \tag{4-8}$$

Acoustic termination at the outlet ($p_2^- = 0$) is applied to determine the transmitted pressure p_2^+, easily. Eq. (4-1) – (4-4) and Eq. (4-5) – (4-8) are used to obtain TL and IL as;

$$TL = 20 \log \left[\frac{\left| A + \frac{B}{\rho c} + C\rho c + D \right|}{2} \right] \tag{4-9}$$

$$IL = \frac{(AZ_2 + B + CZ_1Z_2 + DZ_1)}{Z_1 Z_2} \tag{4-10}$$

where Z_1 and Z_2 are the acoustic impedance of the connected system to reduce the noise at the inlet and outlet.

4.4 Steps of the Numerical Solution of the Study

In this study some steps are followed to model the dissipative perforated silencer with VNoise BEM module. Firstly geometrically the silencer has to be designed before analyse. VNoise provides geometry module to model the silencer but this module can but used for simple shape. Single pass perforated silencer geometry is formed in VNoise, but for hybrid silencer a solid model is built using with a computer aided design (CAD) software because of the QWT resonator. However if the solid model is generated in CAD software, direct output file of the CAD software can't be imported to VNoise. Before importing to VNoise, the solid model has to be surface meshed with finite element analysis software such as Nastran. After modelling the silencer with VNoise or importing the meshed geometry built in another program, boundary conditions have to be defined. Because dissipative silencer has absorbing material in which speed of sound and density differ from air, new domain having complex speed of sound and density has to be generated. Generating the new domain, after selecting the type of the material, glass fiber in this study, resistivity of the absorbing material or complex speed of sound and density in the absorbing material have to be inserted. Besides, interface surface between main duct and outer chamber is formed as perforated plate. Using with semi-empirical approach, impedance of the perforated plate is taken into account. After defining the boundary conditions, in order to start the transmission loss analysis the model has to be discretized. If the meshed model is built in another program and true mesh is imported to the VNoise, there is no need to perform any further manipulation on the mesh. Finally, transmission loss analysis is performed for particular frequency interval.

4.5 Properties of Numerical Model

In this study, sufficiency of the VNoise models is examined before whole numerical transmission loss calculation. As mentioned before, discretization is required for the analysis of transmission loss. Changing the parameters of discretization affects numbers of node and panel on the model surface, so the accuracy is changing. One parameter of discretization is number of points per wave. One can select minimum 6 points per wave for an analysis. To observe the effect the number of points per wave, three different analyses are performed. The transmission loss analyses of a simple expansion chamber with three different discretization parameters are performed and transmission loss results are compared in Figure 4-3.

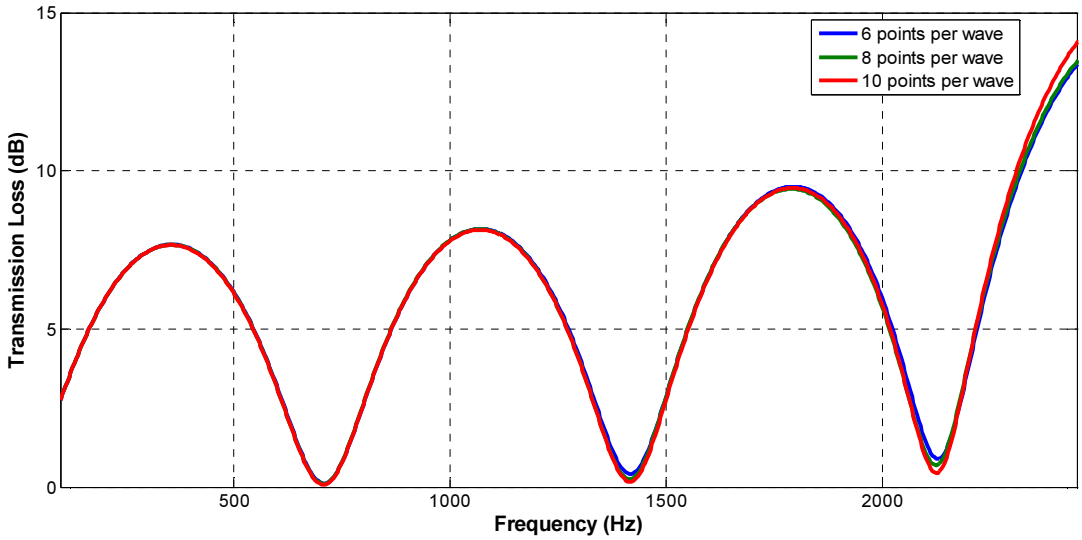

Figure 4-3: Transmission loss of a simple expansion chamber with three different discretized models (6, 8 and 10 points per wave)

First analysis with 6 points per a wave has 1568 nodes and 1344 panels on the silencer surface. In second analysis the point number per a wave is increased to 8, so 2520 nodes and 2268 panels are formed. Final BEM model has 3768 nodes and 3498 panels with 10 points per a wave. Although the node and panel number is increased, the transmission loss is not changing so much. Thus, 6 points per a wave is enough for finding transmission loss of a silencer in VNoise.

CHAPTER 5

TRANSMISSION LOSS MEASUREMENT

This chapter deals with transmission loss measurement methods of an impedance tube illustrating the silencer and the mathematical expressions that are used to calculate the transmission loss from the measured data. Furthermore, in this chapter, transmission loss value found from measurement is compared with that is calculated from analytical and numerical methods.

5.1 Transmission Loss Measurement with Two Load Method [28]

Two-load method is based on calculation of full transfer matrix of an acoustical sample. In this study acoustic sample is silencer transmission loss of which is measured using impedance tube with 4 microphones. Transfer matrix elements are expressed with relation between incident and reflecting waves of source part of tube and incident and reflecting waves passing through the specimen. Transfer matrix is formulated as;

$$\begin{Bmatrix} A_1 \\ B_1 \end{Bmatrix} = \begin{bmatrix} \alpha & \beta \\ \gamma & \delta \end{bmatrix} \begin{Bmatrix} A_2 \\ B_2 \end{Bmatrix} \tag{5-1}$$

where A_1 and B_1 are incident and reflecting waves at the source part of the impedance tube, respectively. Similarly, A_2 and B_2 are incident and reflecting waves at the receive part of the impedance tube, respectively. Incident and reflecting waves of the impedance tube are shown in Figure 5-1.

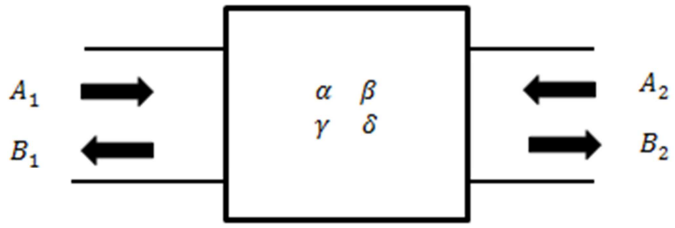

Figure 5-1: Transfer matrix between incident and reflecting waves

The transmission loss of the silencer is expressed as;

$$TL = 20 \log|\alpha| \tag{5-2}$$

Two-load method should contain two solutions with variation of boundary conditions in the end of the impedance tube, i.e. open ended and close ended terminations. Therefore, incident and reflecting waves formulation is represented with including the two ended termination as;

$$\begin{Bmatrix} A_{1O} \\ B_{1O} \end{Bmatrix} = \begin{bmatrix} \alpha & \beta \\ \gamma & \delta \end{bmatrix} \begin{Bmatrix} A_{2O} \\ B_{2O} \end{Bmatrix} \tag{5-3}$$

$$\begin{Bmatrix} A_{1C} \\ B_{1C} \end{Bmatrix} = \begin{bmatrix} \alpha & \beta \\ \gamma & \delta \end{bmatrix} \begin{Bmatrix} A_{2C} \\ B_{2C} \end{Bmatrix} \tag{5-4}$$

where “o” and “c” expressions used in subscripts denote open ended and close ended terminations, respectively. Using Eq. (5-3) and Eq. (5-4), the solution, α, is expressed as;

$$\alpha = \frac{A_{1O}B_{2C} - A_{1C}B_{2O}}{A_{2O}B_{2C} - A_{2C}B_{2O}} \tag{5-5}$$

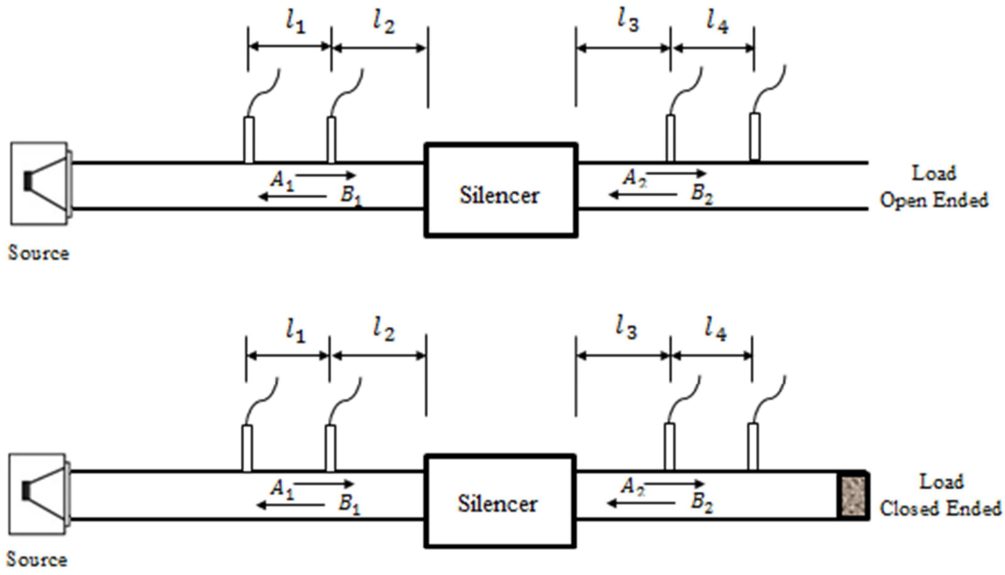

Figure 5-2: Schematic view of measurement setup of two load method

The sound pressures at the corresponding measurement points shown in Figure 5-2 are presented as follows;

$$P_1 = A_1 e^{jk(l_1+l_2)} + B_1 e^{-jk(l_1+l_2)} \tag{5-6}$$

$$P_2 = A_1 e^{jkl_2} + B_1 e^{-jkl_2} \tag{5-7}$$

$$P_3 = A_2 e^{-jkl_3} + B_2 e^{jkl_3} \tag{5-8}$$

$$P_4 = A_2 e^{-jk(l_3+l_4)} + B_2 e^{jk(l_3+l_4)} \tag{5-9}$$

Using the Eq. (5-6) – (5-9), the incident and reflecting waves used in transmission loss calculation are represented as;

$$A_1 = \frac{-j}{2}\frac{P_1 - P_2 e^{-jkl_1}}{\sin(kl_1)} e^{-jkl_2} \tag{5-10}$$

$$B_1 = \frac{j}{2}\frac{P_1 - P_2 e^{jkl_1}}{\sin(kl_1)} e^{jkl_2} \tag{5-11}$$

$$A_2 = \frac{j}{2}\frac{P_4 - P_3 e^{jkl_4}}{\sin(kl_4)} e^{jk3} \tag{5-12}$$

$$B_2 = \frac{-j}{2}\frac{P_4 - P_3 e^{-jkl_4}}{\sin(kl_4)} e^{-jk3} \tag{5-13}$$

The incident and reflecting waves can also be expressed as auto and cross spectrum that are collected data at measurement points.

$$A_1 P_1{}^* = \frac{-j}{2}\frac{S_{11} - S_{12} e^{-jkl_1}}{\sin(kl_1)} e^{-jkl_2} \tag{5-14}$$

$$B_1 P_1{}^* = \frac{j}{2}\frac{S_{11} - S_{12} e^{jkl_1}}{\sin(kl_1)} e^{jkl_2} \tag{5-15}$$

$$A_2 P_1{}^* = \frac{j}{2}\frac{S_{14} - S_{13} e^{jkl_4}}{\sin(kl_4)} e^{jkl_3} \tag{5-16}$$

$$B_2 P_1{}^* = \frac{-j}{2}\frac{S_{14} - S_{13} e^{-jkl_4}}{\sin(kl_4)} e^{-jkl_3} \tag{5-17}$$

where $P_1{}^*$ is the conjugate of P_1. S_{11} is the auto-spectrum of measured data at first microphone location, and S_{12}, S_{13} and $S_{14}$are the cross-spectrum between measured data at first and other microphone locations. Therefore, the transmission loss of the silencer located between impedance tubes can be found from following expression;

$$TL = 20\log\left|\frac{\{A_{1O}P_{1O}{}^*\}\{B_{2C}P_{1C}{}^*\} - \{A_{1C}P_{1C}{}^*\}\{B_{2O}P_{1O}{}^*\}}{\{A_{2O}P_{1O}{}^*\}\{B_{2C}P_{1C}{}^*\} - \{A_{2C}P_{1C}{}^*\}\{B_{2O}P_{1O}{}^*\}}\right| \tag{5-18}$$

where “o” and “c” denote open and close end termination.

5.2 Characteristic Impedance and Wavenumber Measurement with Two Load Method

Same test setup with test specimen of filling material instead of silencer is used to obtain characteristic impedance and complex wavenumber of filling material in the absence of mean flow. This test setup depicted in Figure 5-3 is required when acoustic properties of filling material used in dissipative silencer are not known.

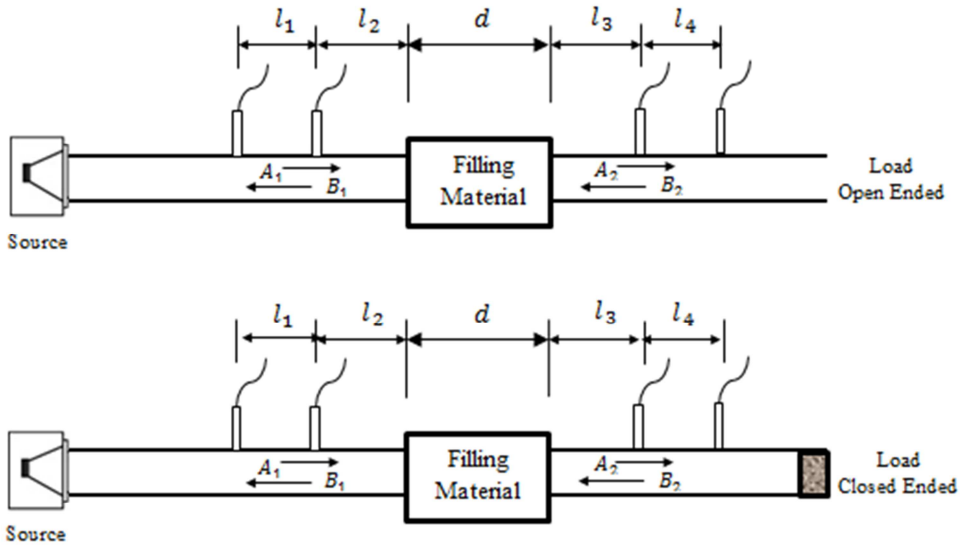

Figure 5-3: Schematic view of test setup with filling material test specimen

In transfer matrix method, not only transmission loss is predicted, but four pole parameters are also found, so the elements of transfer matrix are used to calculate characteristic impedance and complex wavenumber. Song and Bolton [29] present a study in which using with four pole parameters of transfer matrix are used to obtain acoustic properties of absorbing material.

$$\begin{Bmatrix} A_{1O} \\ B_{1O} \end{Bmatrix} = \begin{bmatrix} T_{11} & T_{12} \\ T_{21} & T_{22} \end{bmatrix} \begin{Bmatrix} A_{2O} \\ B_{2O} \end{Bmatrix} \tag{5-19}$$

$$\begin{Bmatrix} A_{1C} \\ B_{1C} \end{Bmatrix} = \begin{bmatrix} T_{11} & T_{12} \\ T_{21} & T_{22} \end{bmatrix} \begin{Bmatrix} A_{2C} \\ B_{2C} \end{Bmatrix} \tag{5-20}$$

A_{1o}, A_{2o}, B_{1o}, B_{2o}, A_{1c}, A_{2c}, B_{1c} and B_{2c} can be found using with Eq. (5-10) – (5-17) described in Sec. 5.1. Transfer function elements can also be written following;

$$\begin{bmatrix} T_{11} & T_{12} \\ T_{21} & T_{22} \end{bmatrix} = \begin{bmatrix} \cos(\tilde{k}d) & j\tilde{\rho}\tilde{c}\sin(\tilde{k}d) \\ j\sin(\tilde{k}d)/\tilde{\rho}\tilde{c} & \cos(\tilde{k}d) \end{bmatrix} \tag{5-21}$$

Complex wave number is calculated from the related elements of the transfer function as;

$$\tilde{k} = \frac{1}{d}\cos^{-1} T_{11} \tag{5-22}$$

or

$$\tilde{k} = \frac{1}{d}\sin^{-1}(\sqrt{T_{12}T_{21}}) \tag{5-23}$$

and the characteristic impedance of the absorbing material is expressed as;

$$\tilde{\rho}\tilde{c} = \sqrt{\frac{T_{12}}{T_{21}}} \tag{5-24}$$

and also complex speed of sound and density in the domain of absorbing material are formulated using with $\tilde{k}$ and $\tilde{\rho}\tilde{c}$.

$$\tilde{c} = \frac{2\pi f}{\tilde{k}} \tag{5-25}$$

$$\tilde{\rho} = \frac{\tilde{\rho}\tilde{c}}{\tilde{c}} \tag{5-26}$$

5.3 Experimental Test Setup

An impedance tube test setup is used to measure the transmission loss of a silencer with two microphones at four different positions, a sound source and digital frequency analysis device in the absence of mean flow. Schematic of the experimental test setup is shown in Figure 5-4.

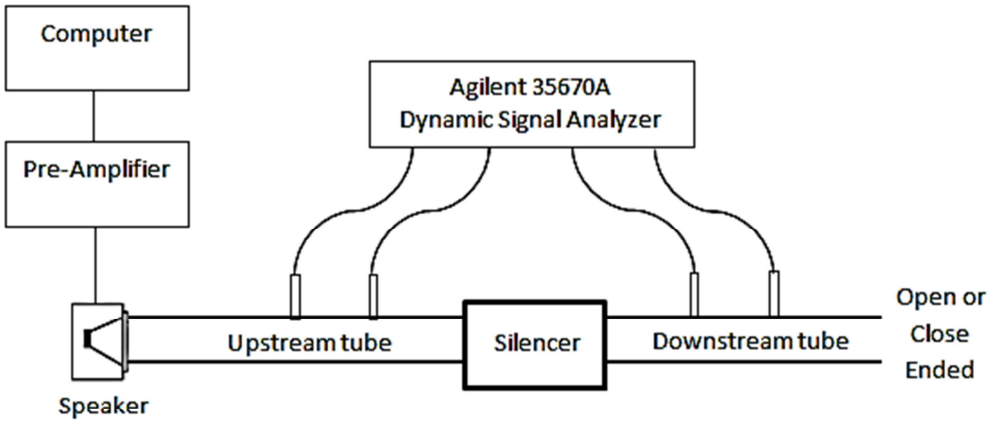

Figure 5-4: Schematic view of experimental test setup

Upstream and downstream tubes are located in front of a speaker which is covered with housing. Silencer is mounted between the upstream and downstream tubes. PCB Piezotronics 1/4 inch condenser microphones (serial numbers: 30735 and 30740) are positioned onto the tubes shown in Figure 5-4. Experimental test setup instruments are shown in Figure 5-5. Agilent 35670A Dynamic Signal Analyzer is used to collect data measured by microphones. Auto-spectrum and cross-spectrum are determined by using the signal analyzer. Pink noise is generated by a computer that connected to a loudspeaker pre-amplifier card driving the speaker. The signal analyzer is adjusted to measure sound pressure at 0-3200 Hz. Resolution is selected 800 lines, so the frequency interval of measurement is 4 Hz. Record length is automatically adjusted to 250 ms by the signal analyzer because of selection of the resolution lines and span frequency. The temperature of the test room is measured to calculate the speed of sound before all measurements and is about 25±1 °C.

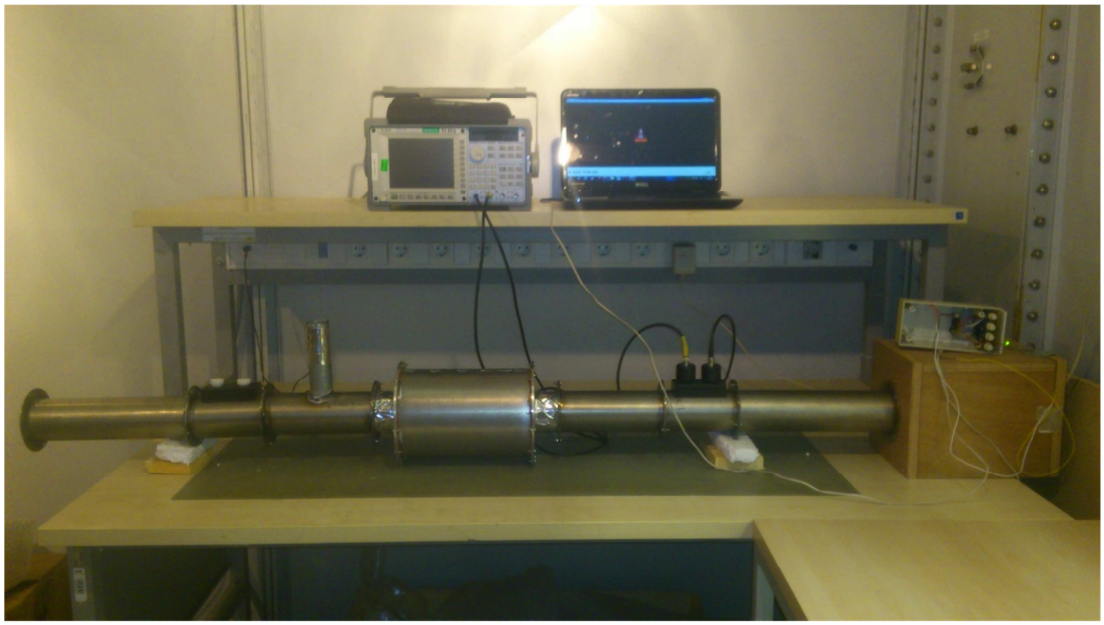

Figure 5-5: The experimental test setup of the study.

5.3.1 Test Setup Specifications [30]

Test setup specifications are important because measurement is valid only when the test setup is constructed properly. Firstly, measurement must be done at upper and lower working frequencies of the impedance tube.

$$f_l < f < f_u \tag{5-27}$$

where, f is the operating frequency, f_l lower working frequency of the tube is limited by the accuracy of the signal processing equipment. First higher order mode (1,0) has cut-off frequency which is f_u upper working frequency of the tube and calculated as following;

$$f_u = 1.84 \frac{c_0}{\pi D} \tag{5-28}$$

where, D is the diameter of the tube. If the operating frequency is below the upper working frequency, the occurrence of non-plane wave mode propagation can be avoided. Spacing between microphones is also an important parameter for accuracy of the measurements. It is recommended to choose as following;

$$s < 0.45 \frac{c_0}{f_u} \tag{5-29}$$

where, s is the spacing between microphones. The lower working frequency, f_l, does not only depend the signal processing equipment, but it is also limited by the spacing between microphones as;

$$f_l = 0.01\frac{c_0}{s} \tag{5-30}$$

Another parameter for plane wave development between the source and the silencer is the tube length. Microphones should be located in the plane wave field. The loudspeakers produce both the plane waves and non-plane modes. So the distance between

The tube should be long enough to cause plane wave development between the source and the sample. These non-plane waves fail within a distance about three tube diameters from the sources. So, microphones should be locates no closer to the source than three tube diameters.

Microphone diameter should be less than 20% of the spacing between two microphones. Besides, the working frequency is dependent on the diameters of the microphones. ASTM E-1050 [31] suggests the following Table 5-1 for relation between diameter of the microphones and the working frequencies;

Table 5-1: Recommended maximum frequency based on microphone diameters

Nominal Diameter (in.)	Diaphragm Diameter (mm)	Maximum Frequency (Hz)
1	22.70	3000
½	12.2	5600
¼	5.95	11 500

The microphones should be mounted to the interior surface of the tube shown in Figure 5-6. The recess between the microphone and surface of the tube is necessary, but it should be as small as possible and be identical for all microphone mountings.

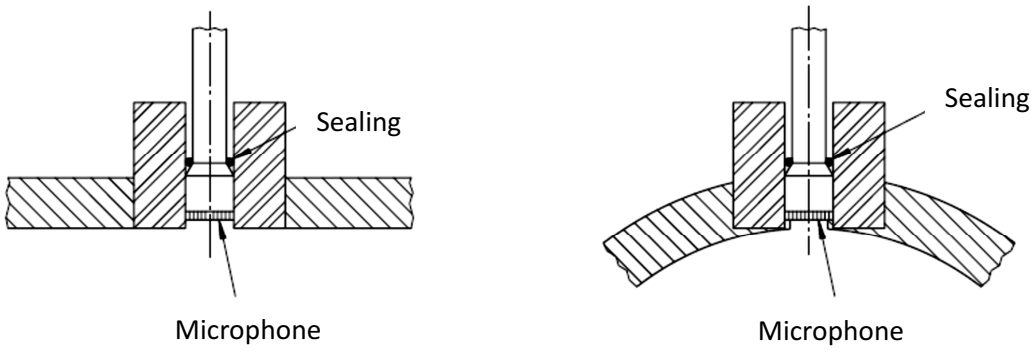

Figure 5-6: Two examples of typical microphone mounting

When using more than one microphone mounting hole for one microphone, the hole not in use must be sealed to maintain smooth surface of the tube.

Speed of sound and air density estimation is important for the accuracy of the measurement. So, before the measurements they shall be determined. Both speed of sound, c_0, and air density, ρ, dependent on the temperature of the tube air and calculated from;

$$c_0 = 343.2\sqrt{T/293} \tag{5-31}$$

$$\rho = \rho_0 \frac{p_a T_0}{p_0 T} \tag{5-32}$$

where T is the temperature, in kelvin, p_a is the atmospheric pressure, in kPa, $T_0 = 293\ K$, $p_0 = 101.325\ kPa$ and $\rho_0 = 1.186\ kg/m^3$. The wavelength is calculated from;

$$\lambda = \frac{c_0}{f} \tag{5-33}$$

5.3.2 Calibration of the Microphones

Transfer function is the complex ratio of the acoustic pressure measured by microphones. So, any conflict of the amplitude or phase responses between two microphones causes the accuracy of the transfer function measurement. Therefore, calibration of the two microphones is required to handle this accuracy problem. The following sequence of the measurements provides correcting the measured data. [31]

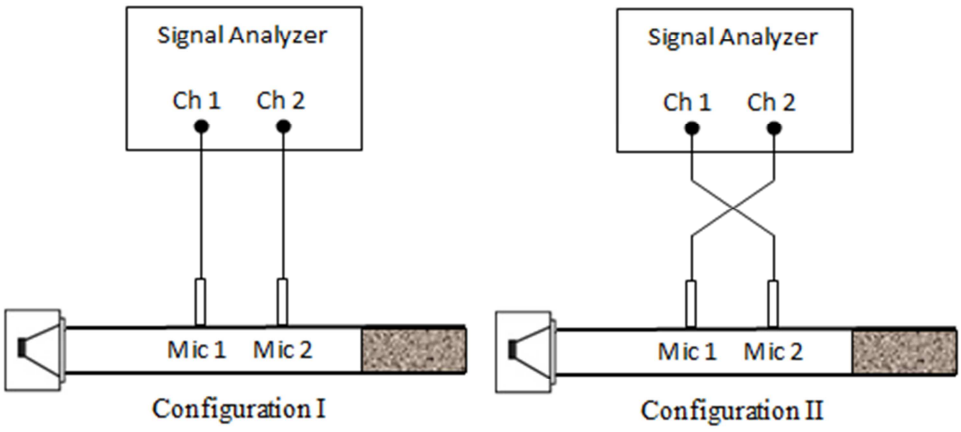

Figure 5-7: Configuration for calibration of the microphones

To obtain the most accurate correction factor highly absorptive specimen should be placed in the tube to prevent the acoustic reflections. Measurement of the transfer function H_{12}^{I} is done in

Configuration I (standard configuration). After that two microphones are interchanged as shown in Figure 5-7 and $H_{12}{}^{II}$ is measured. Calculation of the calibration factor H_c is expressed as;

$$H_c = \sqrt{\frac{H_{12}{}^{I}}{H_{12}{}^{II}}} \tag{5-34}$$

$$H_{12}{}^{I} = \frac{S_{12}{}^{I}}{S_{11}{}^{I}} \tag{5-35}$$

$$H_{12}{}^{II} = \frac{S_{12}{}^{II}}{S_{11}{}^{II}} \tag{5-36}$$

where, $S_{12}{}^{I}$ and $S_{11}{}^{I}$ are cross-spectrum of microphone 1 and microphone 2, and auto-spectrum of microphone 1 in Configuration I, respectively. Similarly, $S_{12}{}^{II}$ and $S_{11}{}^{II}$ are cross-spectrum of microphone 1 and microphone 2, and auto-spectrum of microphone 1 in Configuration II, respectively.

When measuring the transmission loss of a silencer, microphones are placed in Configuration I. Uncorrected transfer function $\hat{H}_{12}$ is measured and correction is applied this value in using

$$H_{12} = \frac{\hat{H}_{12}}{H_c} \tag{5-37}$$

where H_{12} is the corrected transfer function.

5.4 Transmission Loss Measurements

In order to verification of the test setup, transmission losses of simple expansion chamber, perforated reactive silencers with different perforated tube, dissipative silencer and hybrid silencer with indicated perforated tube are determined by using Two-Load Method described in Section 3.1. The results obtained from these experiments are compared with analytical and numerical methods.

5.4.1 Simple Expansion Chamber

First experiment of transmission loss determination is made with simple expansion chamber that is the main element of the dissipative perforated silencer and is presented in Figure 5-8. The diameters of the chamber and inlet-outlet ducts are 164 and 76 mm, respectively. The length of the chamber is 300 mm. These dimensions are used for all expansion chambers of reactive, dissipative and hybrid silencer investigated in this study.

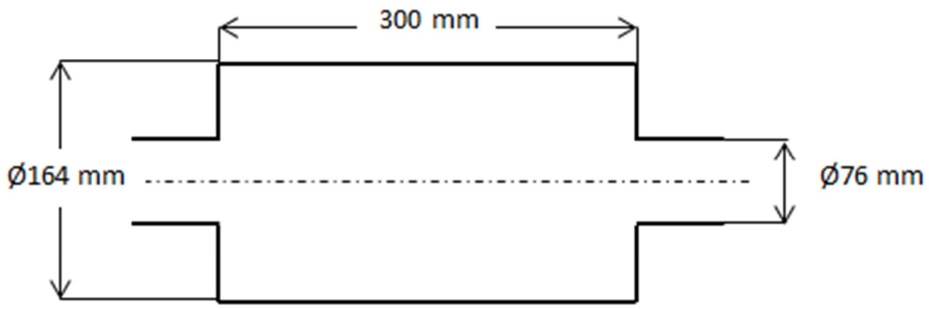

Figure 5-8: The schematic view of simple expansion chamber

Test setup is established considering specifications mentioned in Section 5.3.1. Microphone spacing, s, is taken 50 mm for both upstream and downstream impedance tubes. Upper and lower frequencies are calculated from Eq. (5-28) and Eq. (5-29) to avoid the occurrence of non-plane wave mode propagation in the tube. The upper and lower frequencies of this experiment tube with 76 mm inner diameter are approximately 2645 and 70 Hz, respectively.

The microphone calibration is employed by following the procedure described in section 5.3.2 before the measurement to reduce the experimental errors. The amplitude and phase of the calibration factor between two microphones are presented in Figure 5-9 and Figure 5-10, respectively. Magnitude and phase differences between microphones are so small, and the mismatch between the microphones is inside the tolerable limits.

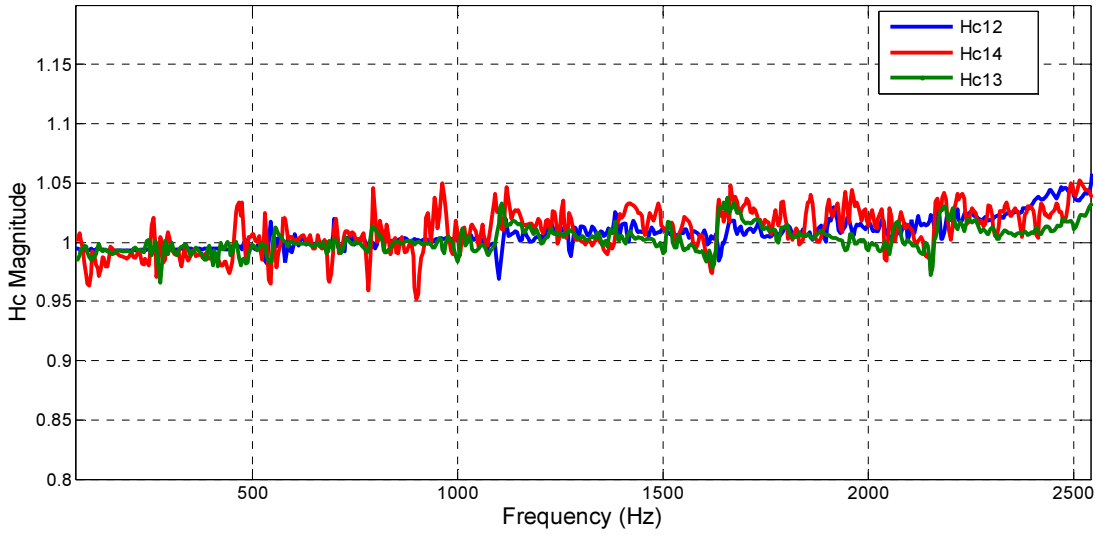

Figure 5-9: Magnitude of the calibration factor between microphones

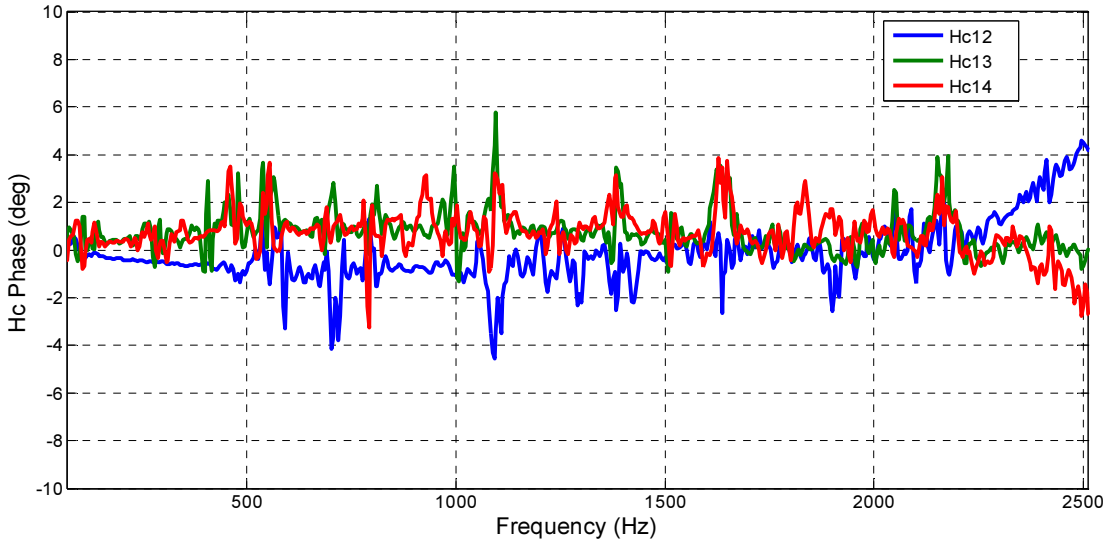

Figure 5-10: Phase of the calibration factor between microphones

Transmission loss of the simple expansion chamber predicted from BEM solution and analytical formulation is compared with experimental results in Figure 5-13. Experiment setup and BEM model of the simple expansion chamber are presented in Figure 5-11 and Figure 5-12, respectively. The results from both BEM solution and experiment are agreed with each other. On the other hand, at high frequencies, after 2000 Hz, the line of transmission loss calculated from 1D analytical method has a deviation. Thus, even for a simple expansion chamber model 1D analytical method would be inadequate. There are resonance frequencies of corresponding length and circumference of expansion chamber, approximately 580 Hz and 700 Hz, respectively.

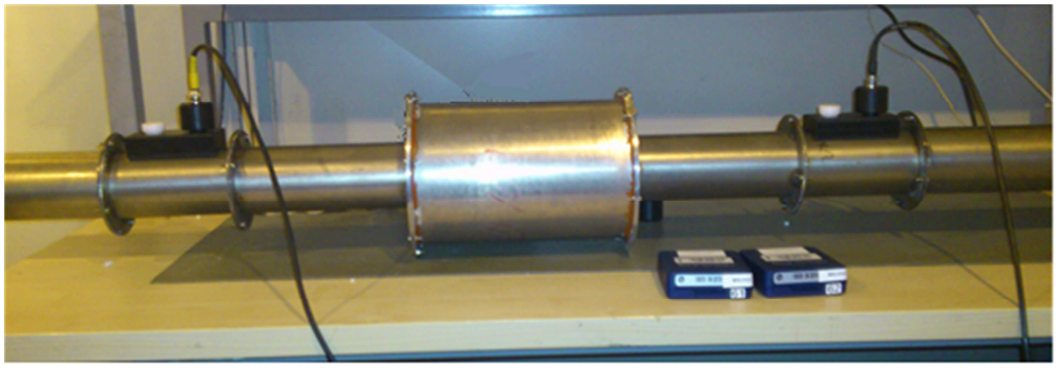

Figure 5-11: Test setup of the expansion chamber

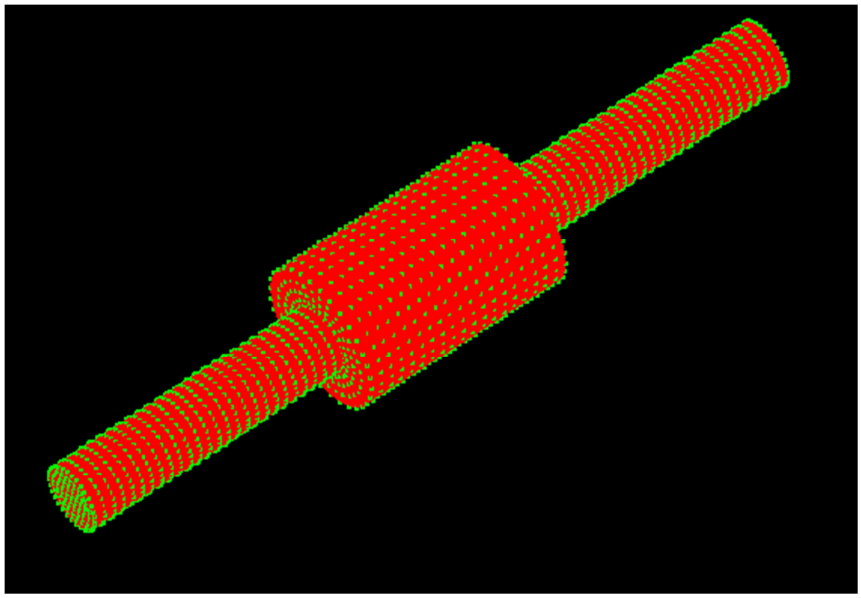

Figure 5-12: BEM model of the simple expansion chamber

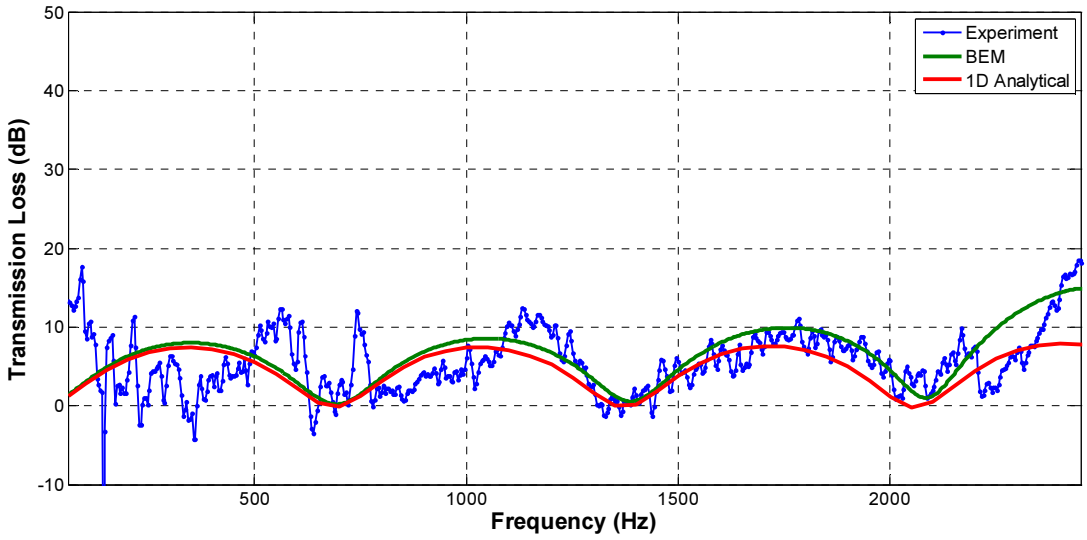

Figure 5-13: Transmission Loss of simple expansion chamber

5.4.2 Reactive Perforated Silencer

In this section various perforated silencers are considered and transmission loss comparison of these perforated silencers is investigated. Four perforated tubes with different porosities, hole diameters and hole arrays are produced by fast prototype printer. Besides, a stainless steel tube that is same as one of these prototypes is manufactured to verify the experiments made with prototype tubes. The schematic view of reactive perforated silencer is figured in Figure 5-14.

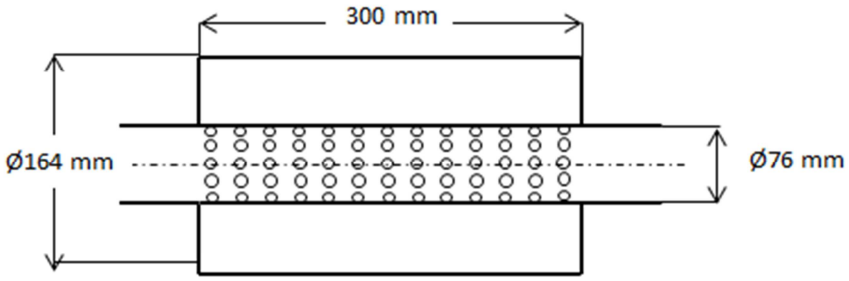

Figure 5-14: The schematic view of reactive perforated silencer.

The inner diameter of the tubes is identical with each other and same as diameter of the simple expansion chamber duct. The thickness of tubes is also identical and 1 mm. The length of tubes is 250 mm and tubes are fit into the expansion chamber. The pictures of the perforated tubes are presented in Figure 5-15. The perforation properties are added to the BEM model of the expansion chamber and transmission loss is predicted for each sample.

a)

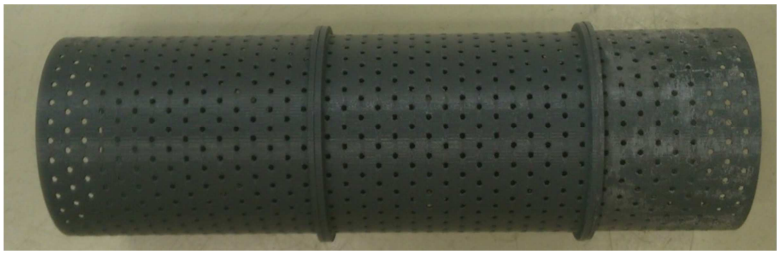

b)

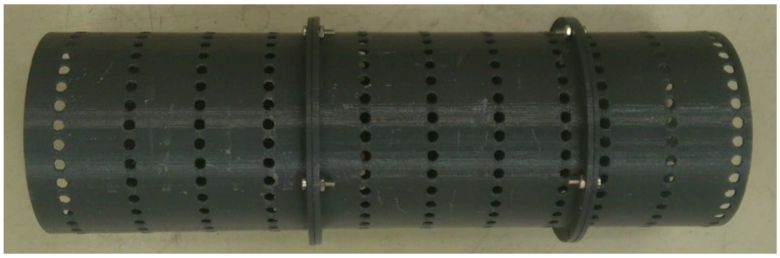

c)

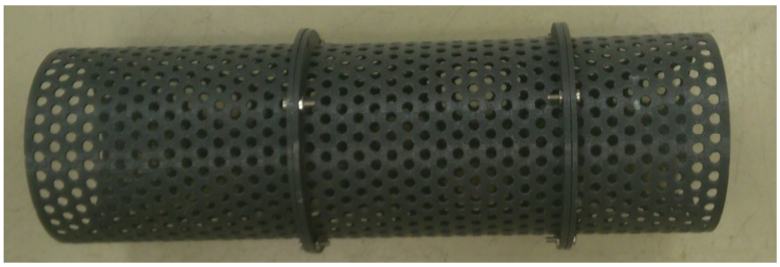

d)

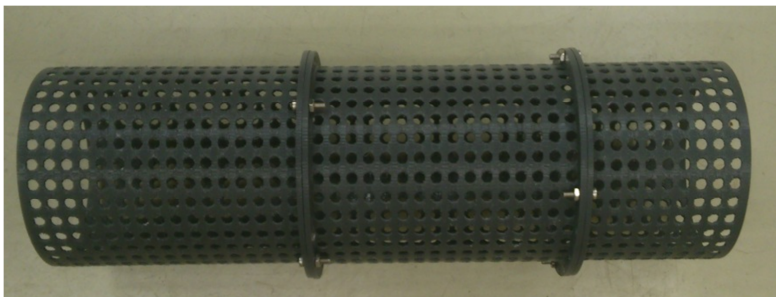

Figure 5-15: The picture of perforated tubes a) d_h = 2 mm and ϕ = 7.2% staggered array b) d_h = 4 mm and ϕ = 7.2% straight array c) d_h = 4 mm and ϕ = 28.8% staggered array d) d_h = 4 mm and ϕ = 28.8% straight array

First perforated tube has 2 mm diameter holes and 7.2% porosity. With second perforated tube, the porosity is kept same as first one, while the hole diameter is changed and doubled. Thus, the effect of the hole diameter on transmission loss can be observed. In third perforated tube the hole diameter remain 4 mm, whereas the porosity is increased to 28.8%. Thus, the effect of porosity is examined with the comparison of transmission loss of silencer with second and third perforated tubes. Besides, the difference between perforation with staggered and straight array is examined with third and fourth perforated tubes that have same porosity and hole diameter. Transmission loss of the each reactive perforated silencer with these samples predicted by numerically, analytically and experimentally is presented between Figure 5-16-Figure 5-19. The perforated tubes are mounted in the simple expansion chamber shown in Figure 5-11. The analytical method would be inadequate for reactive perforated silencer as well as for simple expansion chamber.

The perforation effects arise after 1500 Hz and each perforation has several effects on transmission loss. The presence of perforation increases the transmission loss of silencer after 1500 Hz. Figure 5-20 indicates that dome frequency is chanced by hole diameter. For example, the dome of silencer ($d_h = 2$ and $\phi = 7.2\%$) is divided in two when the hole diameter is doubled while the porosity is kept same. Besides, frequency of the first peak is shifted to the left. The peaks are disappeared when increasing the porosity while keeping the porosity and transmission loss is lying down the dome frequency.

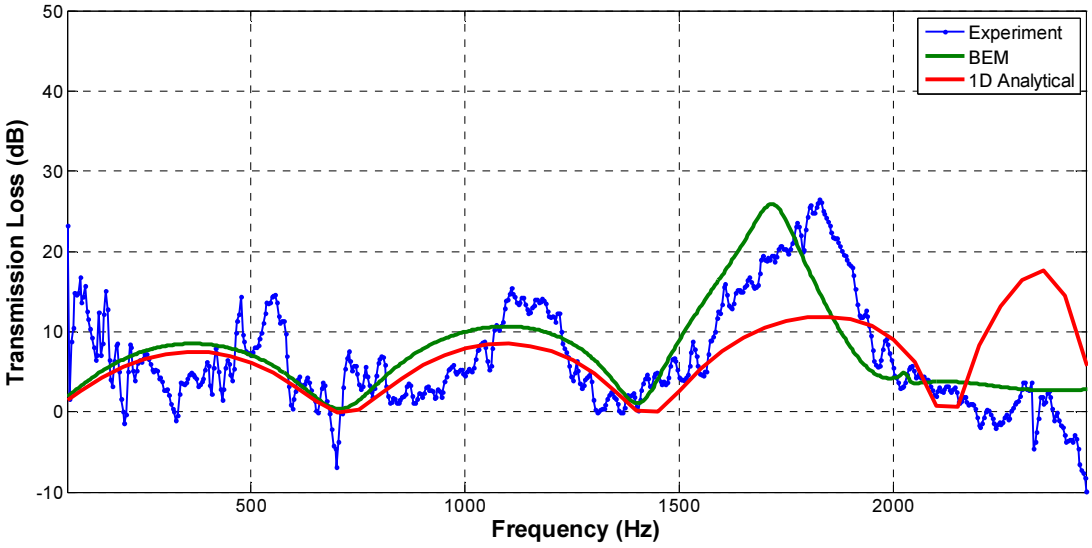

Figure 5-16: Transmission Loss of reactive perforated tube with d_h= 2 mm and ϕ = 7.2%

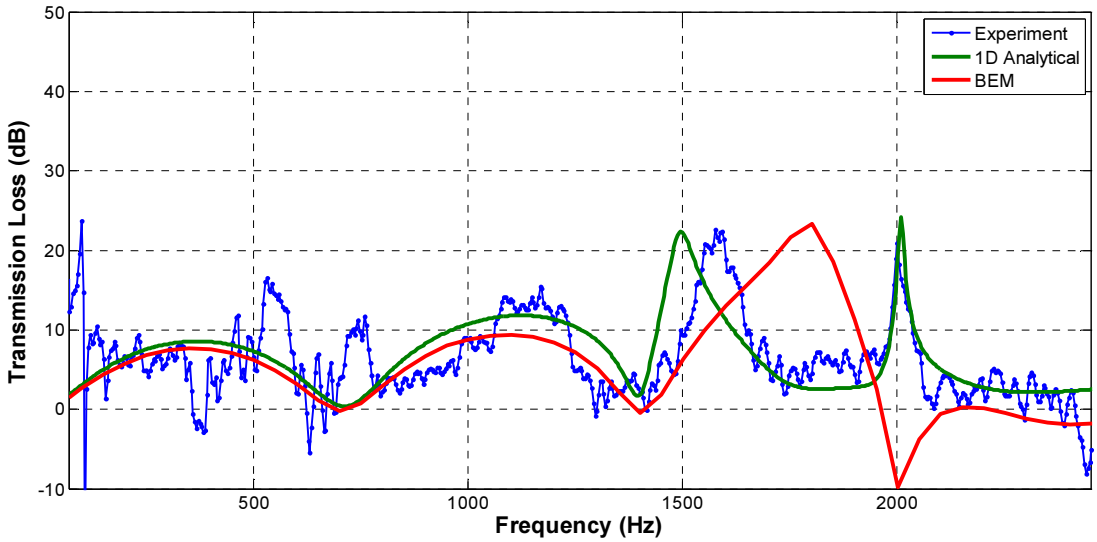

Figure 5-17: Transmission Loss of reactive perforated tube with d_h= 4 mm and ϕ = 7.2%

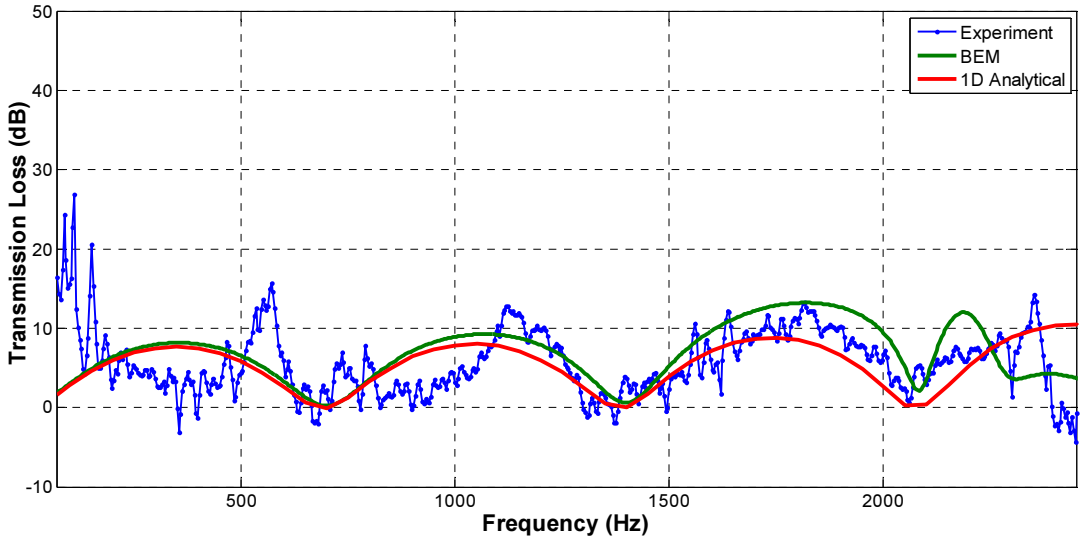

Figure 5-18: Transmission Loss of reactive perforated tube with d_h= 4 mm and ϕ = 28.8% (Staggered array)

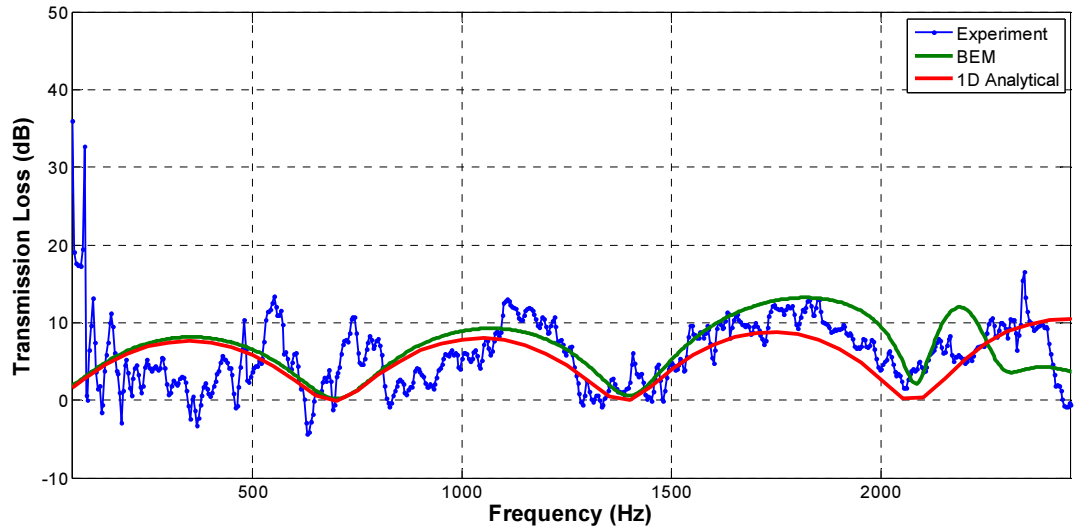

Figure 5-19: Transmission Loss of reactive perforated tube with d_h= 4 mm and ϕ = 28.8% (Straight array)

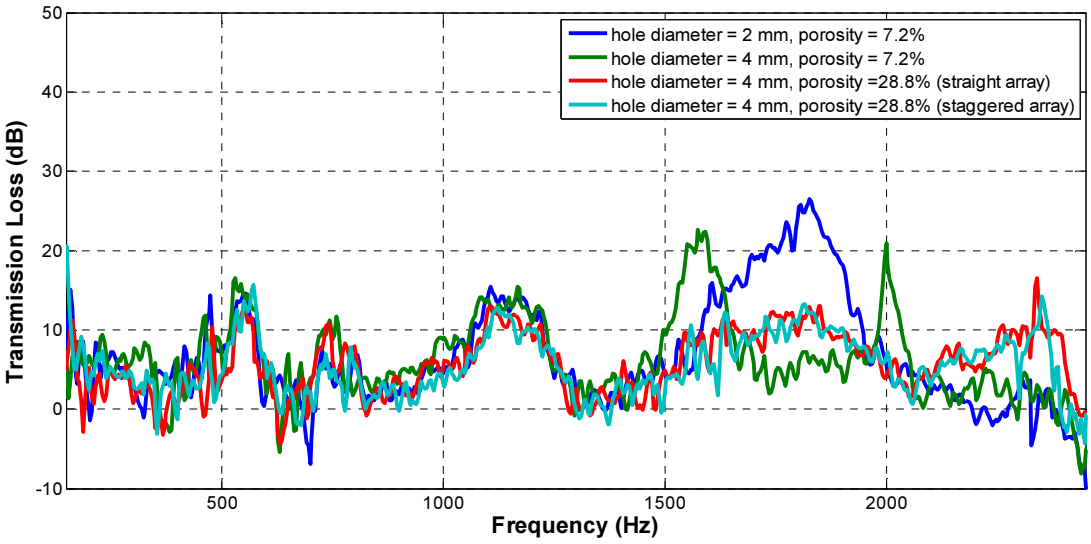

Figure 5-20: Transmission Loss of reactive perforated silencers (Experiment)

After comparing the samples produced with fast prototype printer, a stainless steel perforated tube that has same dimension as third sample is produced to verify the these prototypes. The picture of the stainless steel tube is presented in Figure 5-21. Transmission loss of the tube is also predicted by using same test setup. The numerical and analytical solutions of the tube are same as that of prototype sample. The comparison of transmission loss of the prototype and stainless steel tube is presented in Figure 5-22.

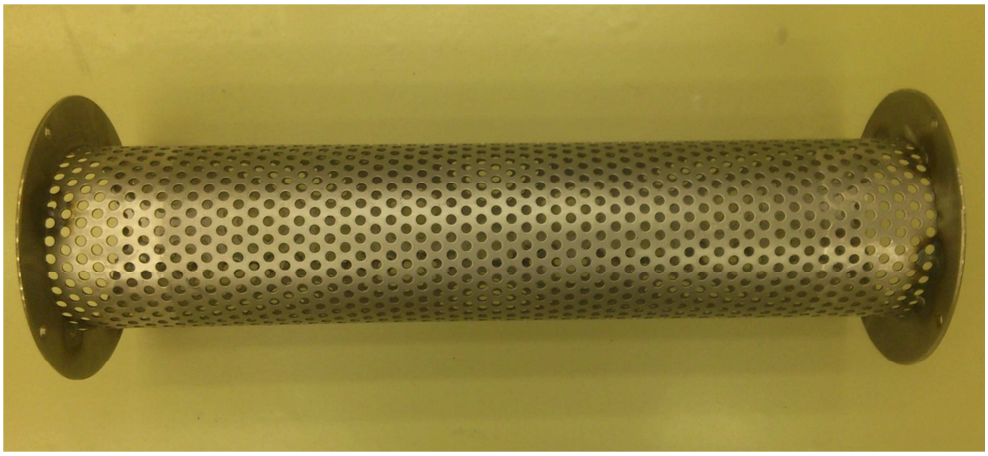

Figure 5-21: Stainless steel perforated tube with d_h= 4 mm and ϕ = 28.8%

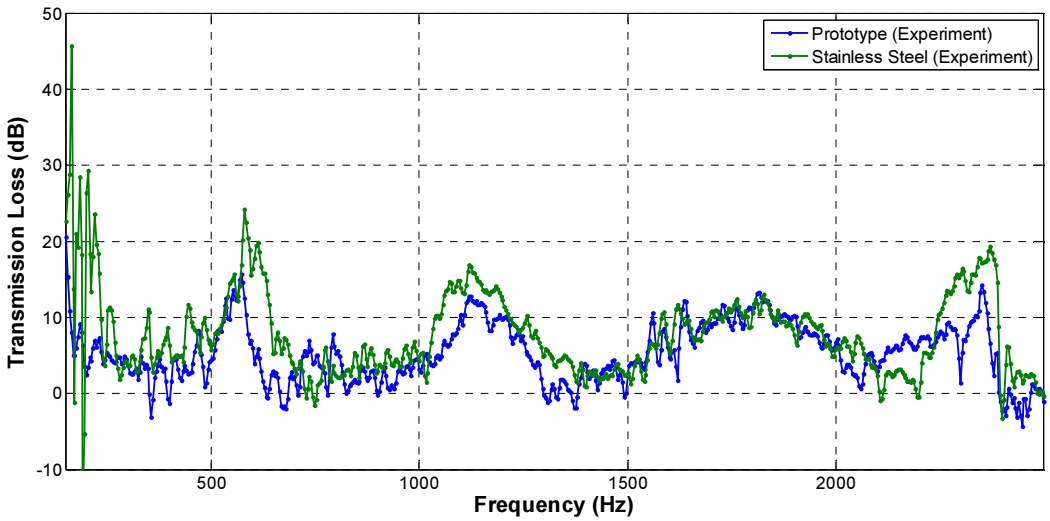

Figure 5-22: Transmission loss of stainless steel tube and third prototype sample with d_h= 4 mm and ϕ = 28.8%

Transmission loss of prototype sample is similar to stainless steel especially the frequency ranges of them are agreed with each other. Thus, the samples produced by fast prototype printer can be used to make experiment of a silencer design before the final product. In this study, the reactive silencer with stainless steel perforated tube is used in following experiments because it is more applicable to use in real case.

5.4.3 Dissipative Perforated Silencer

Dissipative perforated silencer is produced by filling glass fiber into space between perforated tube and expansion chamber. The schematic view of dissipative perforated silencer is demonstrated in Figure 5-23. Transmission loss measurement is carried out for comparing the results of experiment and numerical analysis. However, in numerical solution complex wavenumber and impedance are required to model the fibrous material. So, acoustic properties of absorbing material are predicted by making an experiment and using transfer function method described in Chapter 5.2.

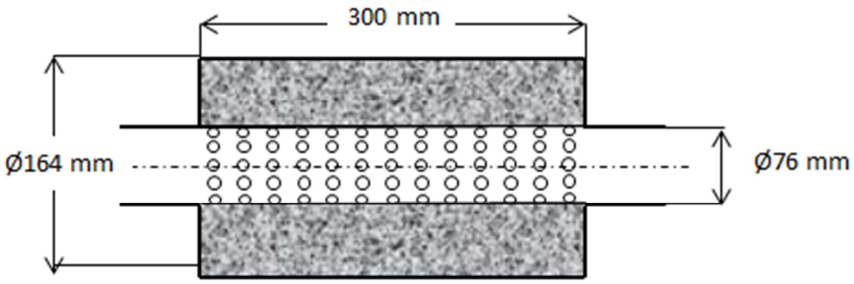

Figure 5-23: The schematic view of dissipative perforated silencer.

Stainless steel tube (d_h= 4 mm and ϕ = 28.8%) is used as perforated tube and predicted transmission loss is presented in Figure 5-24. The results found from BEM model is close to that found from experiment. So, transmission loss of the dissipative perforated silencer with other perforated tubes used in Section 5.4.2 is determined by using only VNoise to eliminate tests. The comparison of transmission loss for each perforated tubes is graphed in Figure 5-25.

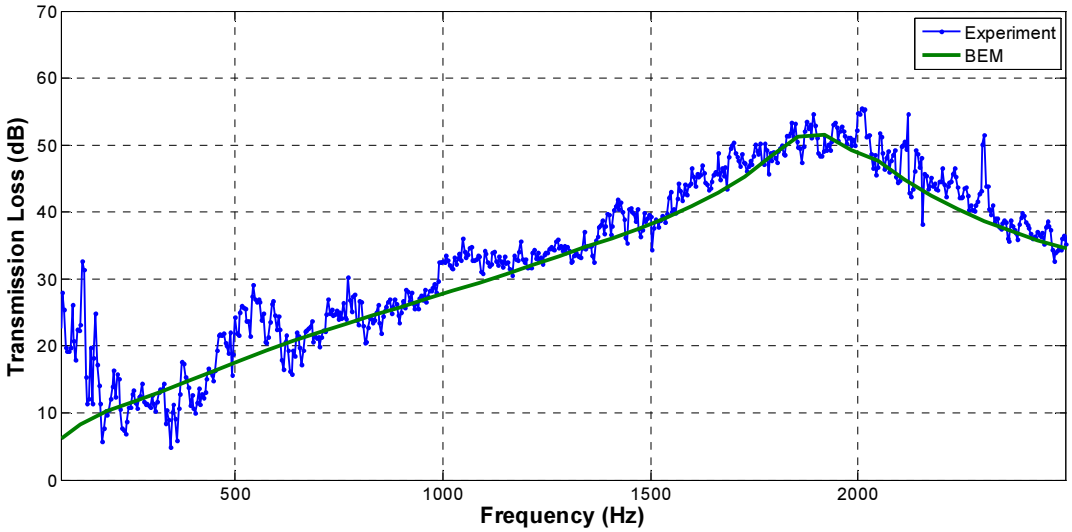

Figure 5-24: Transmission Loss of dissipative perforated silencer (d_h= 4 mm and ϕ = 28.8%)

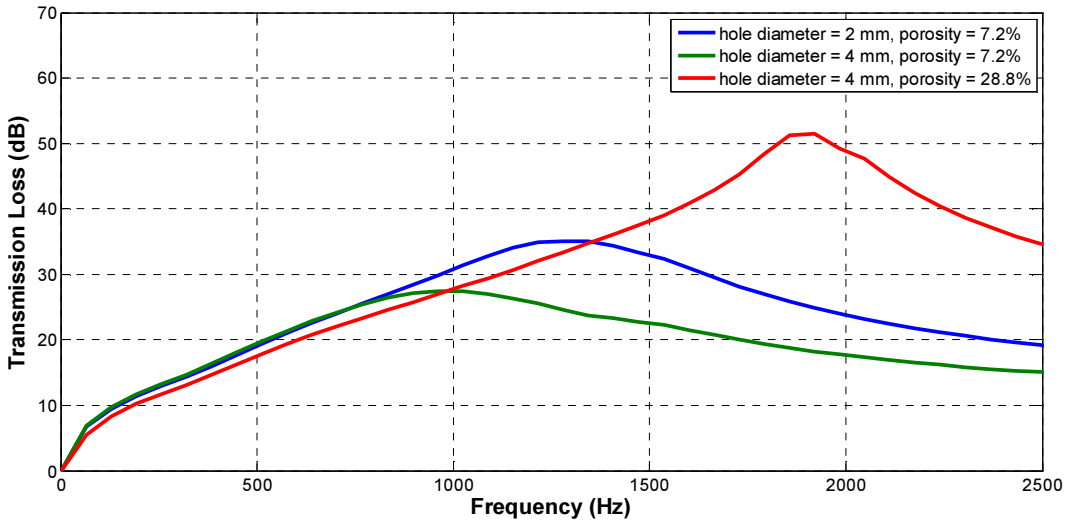

Figure 5-25: Transmission Loss of dissipative perforated silencers (BEM)

The perforation also affects transmission loss of dissipative perforated silencer. However, porosity influences the transmission loss in different way. Figure 5-25 shows that decreasing the porosity from 28.8% to 7.2% (with same hole diameter) decreases transmission loss and shifts the frequency to the left. While, reactive perforated silencer having 7.2% porosity forms peak of transmission loss.

5.4.4 Hybrid Silencer

Hybrid silencer is composed of dissipative perforated silencer (d_h= 4 mm and ϕ = 28.8%) and QWT which is attached to end of the dissipative silencer. QWT is a reactive element and it is used to enhance the attenuation at low frequencies and a specific frequency related to its length. In this study, transmission loss measurements of hybrid silencers with varying length (100 mm, 120 mm and 140 mm) of QWT resonator are examined. The schematic view and of the hybrid silencer are presented in Figure 5-26 and Figure 5-27. The numerical solution is also investigated and the BEM model of the hybrid silencer is shown in Figure 5-28.

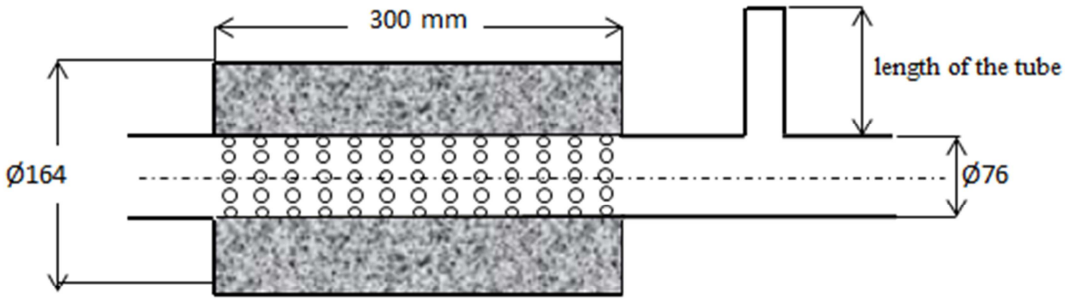

Figure 5-26: The schematic view of hybrid silencer

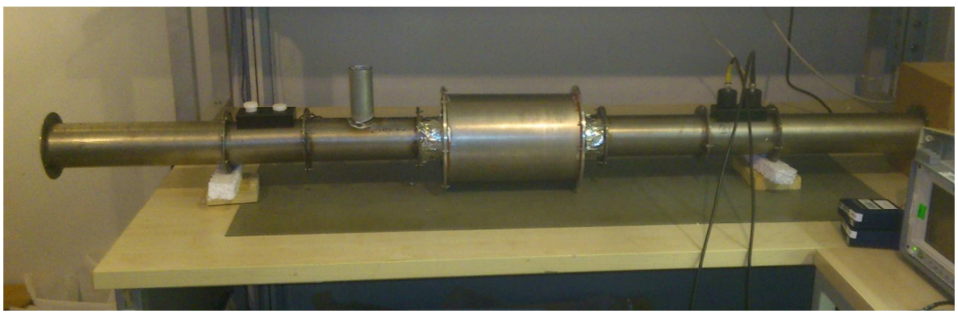

Figure 5-27: The picture of the hybrid silencer

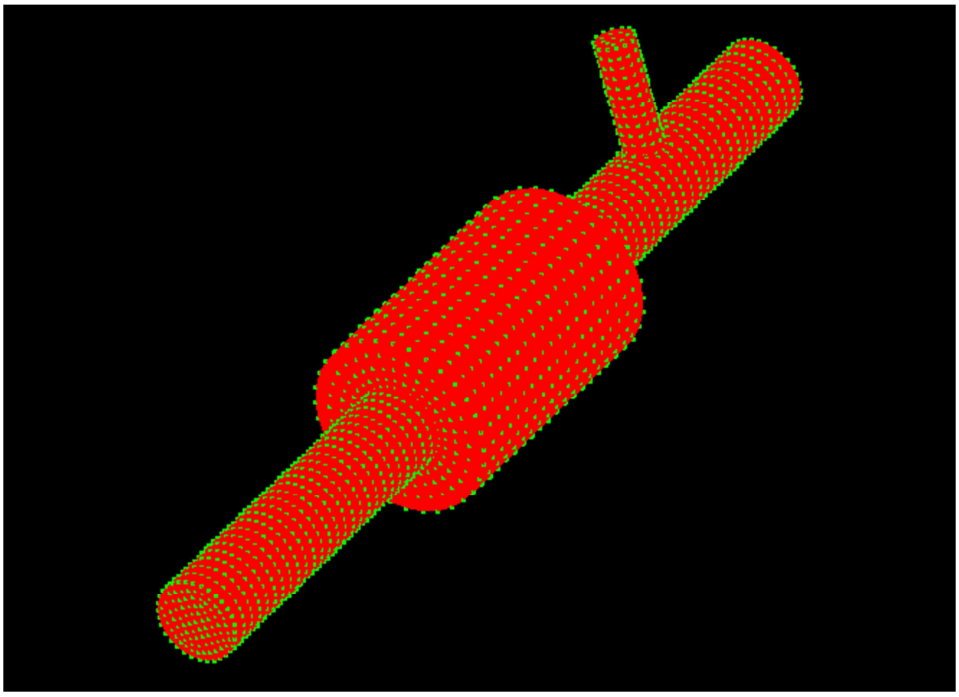

Figure 5-28: BEM model of the hybrid silencer

Hybrid silencers with 100, 120 and 140 mm length of QWT resonator are investigated by numerically and experimentally, and transmission loss graphics are presented in Figure 5-29. The BEM solutions are good agreement with experimental results for all hybrid silencers. At high frequencies, transmission loss values are increased because of dissipative perforated part of the hybrid silencer. At low frequencies, the side branch affects the sound attenuation and transmission loss has a dome at frequency of corresponding tube length. Figure 5-32 indicates difference between the hybrid silencers with varying lengths of QWT. Increasing length of the QWT shifts the frequency to the left. So, the resonance wavelength of QWT is increasing.

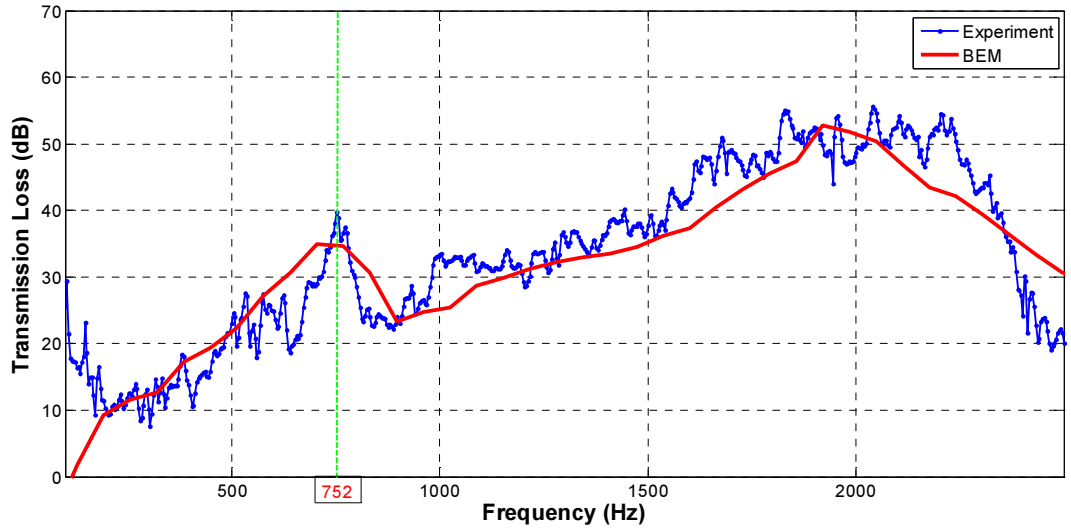

Figure 5-29: Transmission Loss of Hybrid Silencer with 100 mm length of QWT (d_h= 4 mm and ϕ = 28.8%)

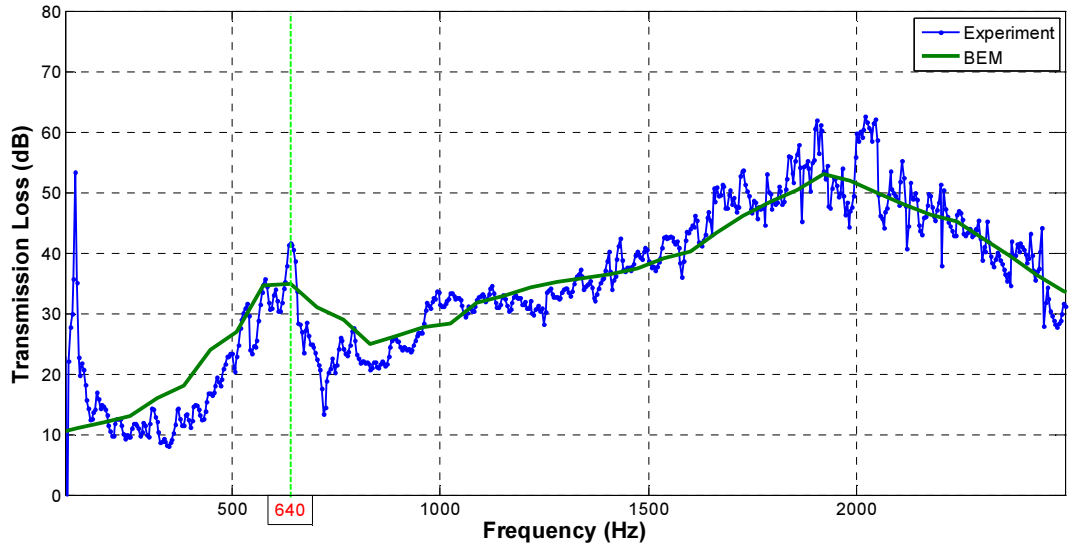

Figure 5-30: Transmission Loss of Hybrid Silencer with 120 mm length of QWT (d_h= 4 mm and ϕ = 28.8%)

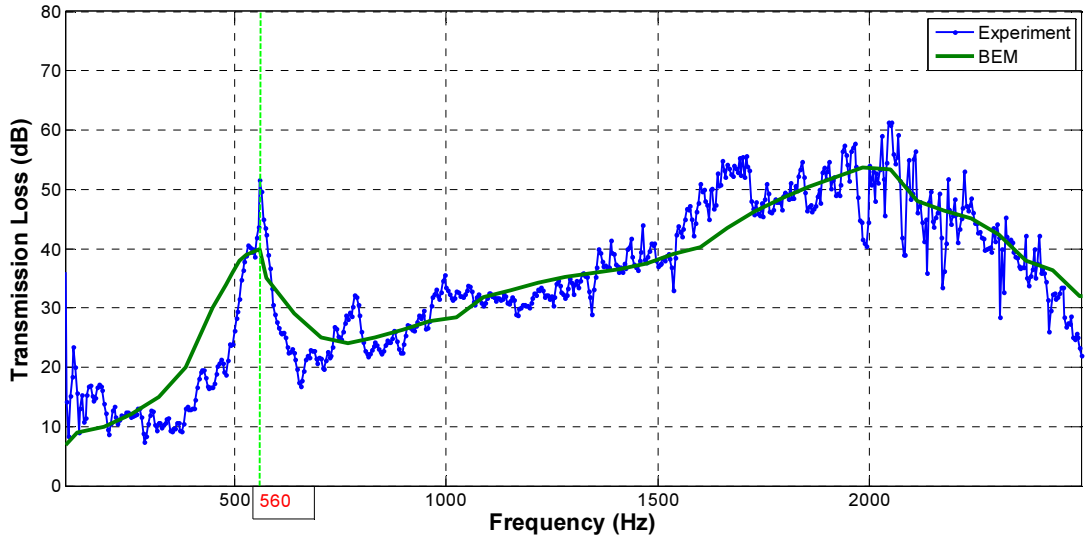

Figure 5-31: Transmission Loss of Hybrid Silencer with 140 mm length of QWT (d_h= 4 mm and ϕ = 28.8%)

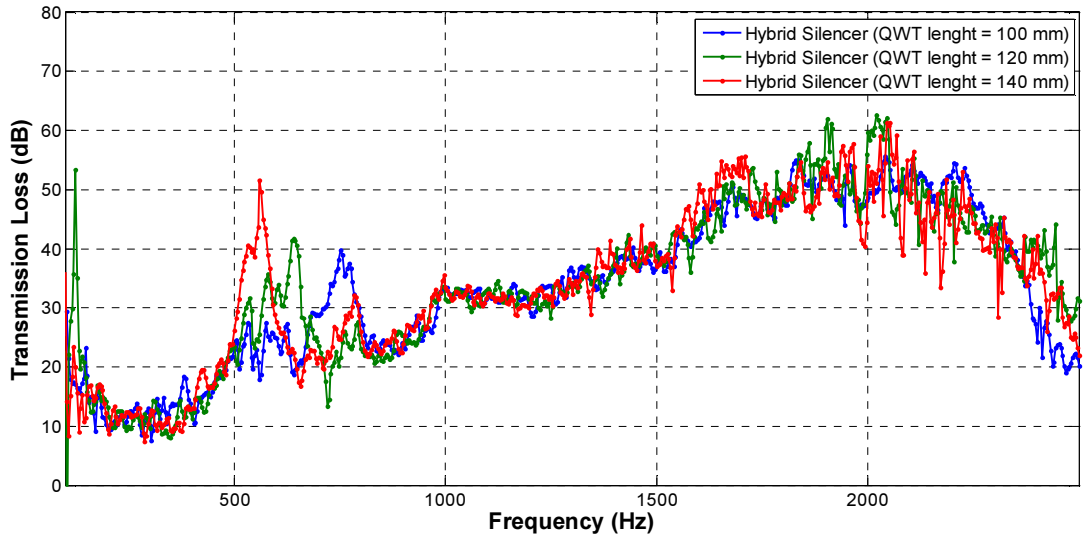

Figure 5-32: Transmission Loss of Hybrid Silencers (Experiment)

The resonance frequencies of QWT resonators shown in Figure 5-29, Figure 5-30 and Figure 5-31 are used to calculate effective lengths of the QWT by using Eq. (3-41). The calculated effective lengths are 115, 135 and 155 mm for 100, 120 and 140 mm lengths of QWT resonator, respectively. Using the effective lengths of side branch, transmission losses of QWT resonator alone are calculated with Eq. (3-43). Transmission loss of hybrid silencer is actually summation of dissipative perforated silencer and QWT resonator alone. Figure 5-33, Figure 5-34 and Figure 5-35 show transmission loss of dissipative perforated silencer, hybrid silencer and QWT alone.

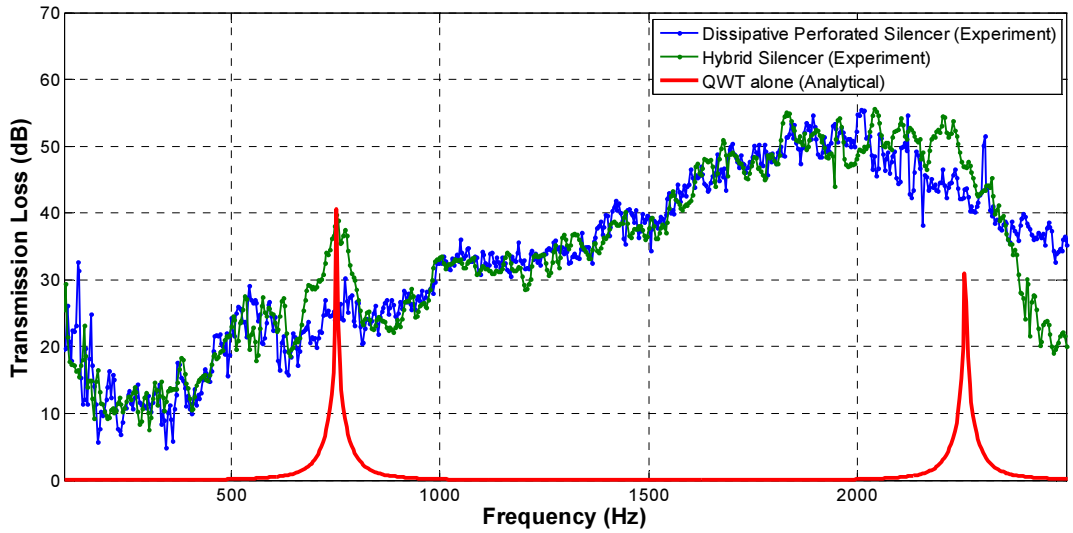

Figure 5-33: Transmission Loss comparison of dissipative perforated tube, hybrid silencer and QWT (QWT length = 100 mm)

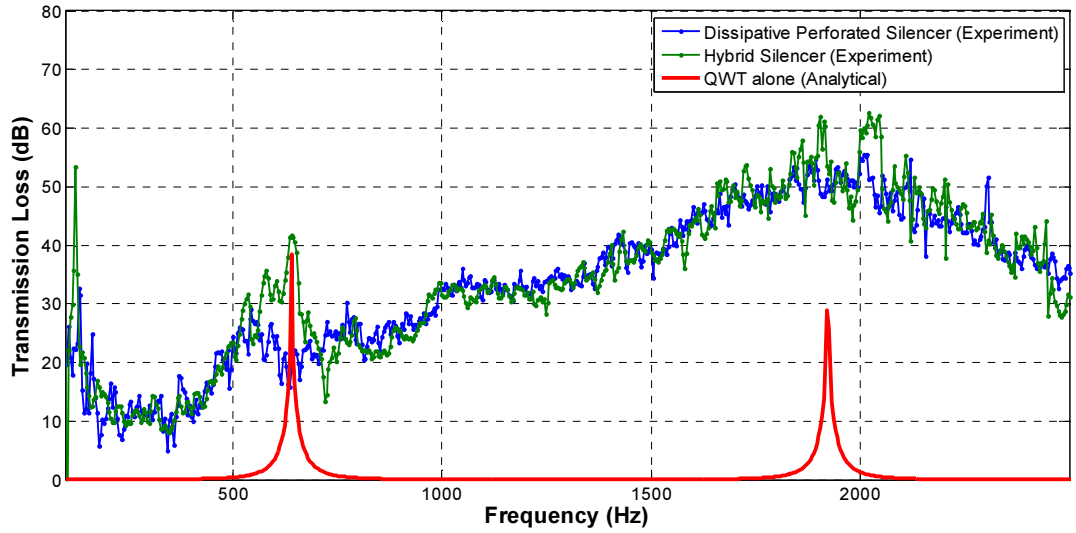

Figure 5-34: Transmission Loss comparison of dissipative perforated tube, hybrid silencer and QWT (QWT length = 120 mm)

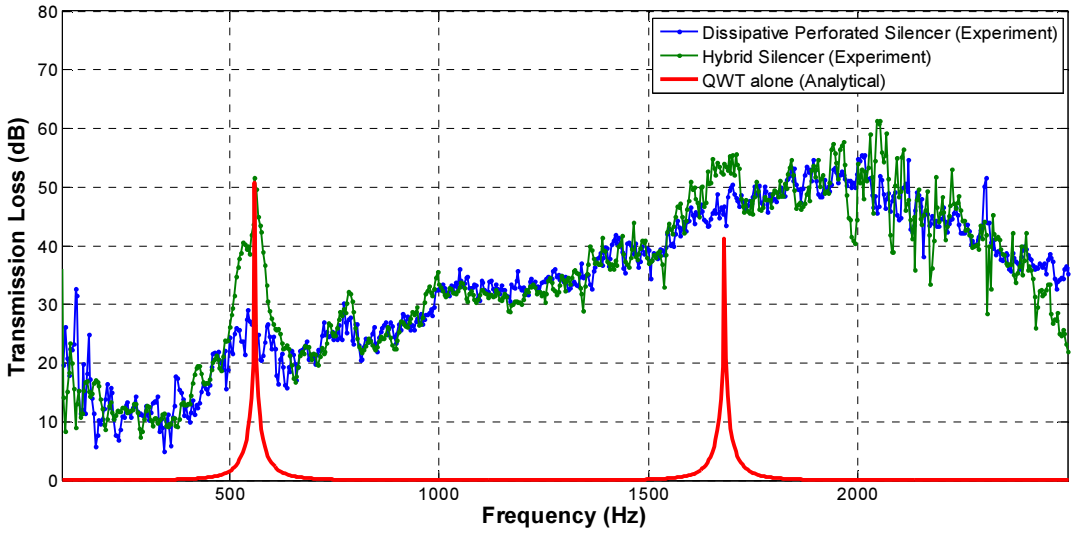

Figure 5-35: Transmission Loss comparison of dissipative perforated tube, hybrid silencer and QWT (QWT length = 140 mm)

CHAPTER 6

CONCLUSION

Acoustical evaluation of hybrid silencer composed of a dissipative perforated silencer and quarter wave tube resonator is carried in this study. Firstly, simple expansion chamber and reactive perforated silencer are investigated to pedict the transmission loss, the main criteria for acoustical characteristics of a silencer, as dissipative perforated silencer is made up of an expansion chamber and perforated tube. Transmission losses of simple expansion chamber and reactive perforated silencer are predicted analytically, numerically and experimentally. Findings for each approach are compared with each other. After comparison of these three methods, it is seen that theoretical solution is inadequate at high frequencies, whereas BEM solution is found to agree with the experimental results. Second investigation is carried to determine the transmission loss of a dissipative perforated silencer. Two experimental setup schemes are established to examine the acoustical characteristics of dissipative perforated silencer. One of the test setup is exploited to predict transmission loss of the silencer as used for simple expansion chamber and reactive perforated silencer. The other one is used to investigate characteristic impedance and wavenumber of filling material making reactive perforated silencer dissipative. Finally, transmission loss of the hybrid silencer is predicted numerically and experimentally. The conclusions are briefly described next.

Characteristic impedance and wavenumber of the absorbing material are obtained using the experimental test setup. Experimentally data are used to determine the acoustic impedance of perforations in contact with the fibrous material and the transmission loss of dissipative silencer. Empirical expressions are also available in this study for determination of acoustic impedance of perforations in contact with air and filling material in the absence of mean flow.

Acoustical properties of the absorbing material measured experimentally and impedance of the perforation are combined to find the transmission loss of silencers. Firstly, the measurement of a simple expansion chamber is performed as the basic element of a silencer is the expansion chamber. Then, the measured transmission loss of reactive perforated silencer having prototype perforated tubes produced with different porosities (%7.2 and %28.8), various hole diameters (2 and 4 mm) and also different hole array pattern (staggered and straight) are compared with the predicted transmission loss by theoretical models. Then, stainless steel perforated tube is produced to see the difference between the prototype and real case. Upon measurement of reactive perforated silencers, the absorbing material is filled around the stainless steel perforated tube to make up the dissipative silencer. The measured transmission loss is also compared to predicted value by BEM. Finally, dissipative silencer and QWT are combined to form a hybrid silencer to attenuate the broadband noise and pure tone. The following conclusions can be drawn for this study:

- One-dimensional analytical solution is inadequate for high frequencies because plane wave assumption is no longer valid at high frequencies.
- The predictions of BEM is agreed with experimental results for all silencer types used in this study, except for near the resonance frequency because of length and circumference of the expansion chamber.
- The prototype perforated tubes produced with rapid prototype printer behave like stainless steel perforated tube, but the transmission loss lines shown in Figure 5-22 slightly differ from each other because of damping properties of materials. Thus, prototypes can be used for tests in the process of product development.

- Transmission loss of dissipative silencer is higher than the reactive perforated silencer. When the absorbing material is used, the multi domes are in the transmission loss spectrum disappear forming a single dome.
- Hybrid silencer provides both attenuation of broadband noise and pure tone together. In addition to this, transmission loss of hybrid silencer is summation of the transmission loss of dissipative silencer and QWT.
- Transmission loss characteristics of all silencer types considered in the study were obtained for no flow conditions. Results still applies for condition with flow as long as the Mach number is less than 0.2.
- Predictions by theoretical models of simple expansion chamber, reactive and dissipative silencer and hybrid silencer are found to agree with experimental results.

This study can be used as a guidance for designing a dissipative or hybrid silencer. Different perforated tubes with changing hole patterns can be produced with rapid prototype printers without much loss in accuracy from the real product.

6.1 Future Work

The impedance test setup can be improved to measure the transmission loss with mean flow. Predictions of theoretical models can also be compared with experimental results for existing the mean flow.

Determination of QWT effective length is difficult for a specific frequency, as the transmission loss of QWT is nearly zero except for that frequency. However, if this hybrid silencer is used in real case, for example to reduce the noise of a fan, the length of the side branch must be selected exactly equal to the quarter wavelength corresponding to the blade passing frequency. To deal with this problem, to find the exact length of the side branch QWT with adjustable mechanism can be produced.

REFERENCES

[1] M. Ohadi and Q. Jianwei, *Thermal Management of Harsh-Environment Electronics,* 2004.

[2] S. Akaike, K. Kikuyama, M. Kitada and K. Kuwayama, "Study of Rotational Noise Reduction for Axial Flow Fan : Analysis and Estimation of Secondary Fan-Noise Component," *JSME International Journal,* vol. 39, pp. 590-596, 1996.

[3] J. Igarashi and M. Toyama, "Fundamentals of Acoustical Silencers (I) Theory and Experiment of Acoustic Low-Pass Filters," University of Tokyo, Tokyo, 1958.

[4] J. W. Sullivan and M. J. Crocker, "Analysis of Concentric Tube Resonators Having Unpartitioned Cavities," *Journal of the Acoustical Society of America,* vol. 64, pp. 207-215, 1978.

[5] J. W. Sullivan, "A Method for Modelling Perforated Tube Muffler Components I. Theory," *Journal of the Acoustical Society of America,* vol. 66, pp. 772-778, 1979.

[6] K. Jayaraman and K. Yam, "Decoupling Approach to Modelling Perforated Tube Muffler Components," *Journal of Acoustical Society of America,* vol. 69, pp. 390-396, 1981.

[7] A. Cummings and I. J. Chang, "Internal Mean Flow Effects on the Characteristics of Bulk-Reacting Liners in Circular Ducts," *Acustica,* vol. 64, pp. 169-178, 1987.

[8] A. Selamet and P. M. Radavich, "The Effect of Length on the Acoustic Attenuation Performance of Concentric Expansion Chambers: An Analytical, Computational and Experimental Investigation," *Journal of sound and Vibration,* vol. 201, pp. 407-426, 1997.

[9] S. N. Gerges, R. Jordan, F. A. Thieme, J. L. Bento Coelho and J. P. Arenas, "Muffler Modeling by Transfer Matrix Method and Experimental Verification," *ABCM,* vol. 27, pp. 132-140, 2005.

[10] C. N. Wang and C. Y. Liao, "Boundary Integral Equation Moethod for Evaluating the Performance of Straight-Through Resonator with Mean Flow," *Journal of Sound and Vibration,* vol. 216, pp. 281-294, 1998.

[11] T. W. Wu, P. Zhang and C. Y. R. Cheng, "Boundary Element Analysis of Mufflers with an Improved Method for Deriving the Four-pole Parameters," *Journal of Sound and Vibration,* vol. 217, pp. 767-779, 1998.

[12] C. J. Young and M. J. Crocker, "Prediction of Transmission Loss in Mufflers by the Finite-Element Method," *Journal of the Acoustic Society of America,* vol. 57, pp. 144-148, 1975.

[13] C. J. Young and M. J. Crocker, "Acoustical Analysis, Testing, and Design of Flow-Reversing Muffler Chamber," *Journal of the Acoustical Society of America,* vol. 60, pp. 1111-1118, 1976.

[14] J. Y. Chung and D. A. Blaser, "Transfer Function Method of Measuring in-duct Acoustic Properties. I. Theory," *Journal of the Acoustical Society of America,* vol. 68, pp. 907-913, 1980.

[15] A. F. Seybert and D. F. Ross, "Experimental determination of acoustic properties using a two-microphone random-excitation technique," *Journal of the Acoustical Society,* vol. 61, pp. 1362-1370, 1977.

[16] Z. Tao and A. F. Seybert, "A Review of Current Techniques for Measuring Muffler Transmission Loss," in *Proceedings of the SAE Noise and Vibration Conference*, 2003.

[17] B. Yousefzadeh, M. Mahjoob, N. Mohammadi and A. Shahsavari, "An Experimental Study of Sound Transmission Loss (STL) Measurement Techniques Using an Impedance Tube," in *Acoustics'08*, Paris, 2008.

[18] L. J. Eriksson, "Higher order mode effects in circular ducts and expansion chambers," *Journal of the Acoustical Society of America,* vol. 68, pp. 545-550, 1980.

[19] B. R. Wyerman, "A theoretical and experimental study of acoustic propagation in multisectioned

circular ducts", Doctoral Thesis submitted to Pennsylvania State Univercity, 1976.

[20] Y. Fan, F. Honarvar, A. N. Sinclair and M. Jafari, "Circumferential resonance modes of solid elastic cylinders excited by obliquely incident acoustic waves," *Acoustical Society of America,* vol. 113, pp. 102-113, 2003.

[21] C. N. Wang, "Numerical Decoupling Analysis of A Resonator with Absorbent Material," *Applied Acoustics,* vol. 58, pp. 109-122, 1999.

[22] L. L. Beranek and I. L. Ver, Noise and Vibration Control Engineering: Principles, John Wiley & Sons, Inc., 1992.

[23] M. E. Delany and E. N. Bazley, "Acoustical properties of fibrous absorbent," *Applied Acoustics,* vol. 3, pp. 105-116, 1970.

[24] I. -J. Lee, A. Selamet and N. T. Huff, "Acoustic impedance of perforations in contact with fibrous material," *Acoustical Society of America,* vol. 119, p. 2785–2797, 2006.

[25] R. Kirby and A. Cummings, "The impedance of perforated plates subjected to grazing gas flow and backed by porous media," *Journal of Sound and Vibration,* vol. 217, pp. 619-636, 1998.

[26] D. A. Bies ve C. H. Hansen, Engineering Noise Control: Theory and Practice, New York: Taylo r& Francis Group, 2009.

[27] Perforated Tubes Modelling [VNoise Application Note 004], 2005.

[28] R. Yunseon and M. Choi, "Transmission Loss Measurement of the Exhaust System Using 4-Micropones with Impedance Tube," in *18th International Congress on*, 2004.

[29] B. H. Song and J. S. Bolton, "A transfer-matrix approach for estimating the characteristic impedance and wave numbers of limp and rigid porous materials," *Acoustic Society of America,* vol. 107, pp. 1131-1152, 2000.

[30] *ISO 10534-2: Determination of sound absorption coefficient and impedance in impedance tubes - Transfer Function Method,* 1998.

[31] *ASTM E 1050: Standard Test Method For Impedance And Absorption of Acoustical Materials Using A Tube, Two Microphones and A Digital Frequency Analysis System.*

[32] M. J. Crocker, Handbook of Noise and Vibration Control, 1 ed., John Wiley & Sons, 2007.

[33] M. L. Munjal, Acoustics of Ducts and Mufflers, NewYork: John Wiley and Sons, Inc., 1987.